Eugene C. Lundquist

NATIONAL ADVISORY COMMITTEE
FOR AERONAUTICS

TECHNICAL NOTE

No. 1368

THEORETICAL AND EXPERIMENTAL DATA FOR A NUMBER OF

NACA 6A-SERIES AIRFOIL SECTIONS

By Laurence K. Loftin, Jr.

Langley Memorial Aeronautical Laboratory
Langley Field, Va.
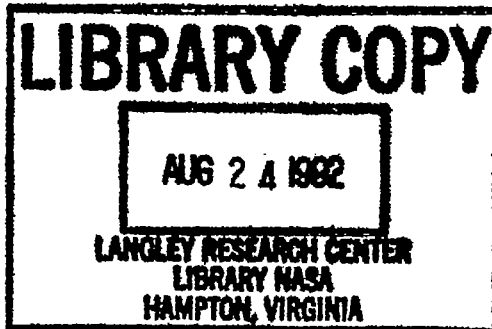
Washington

July 1947

NATIONAL ADVISORY COMMITTEE FOR AERONAUTICS

TECHNICAL NOTE NO. 1368

THEORETICAL AND EXPERIMENTAL DATA FOR A NUMBER OF

NACA 6A-SERIES AIRFOIL SECTIONS

By Laurence K. Loftin, Jr.

SUMMARY

The NACA 6A-series airfoil sections were designed to eliminate
the trailing-edge cusp which is characteristic of the NACA 6-series
sections. Theoretical data are presented for NACA 6A-series basic
thickness forms having the position of minimum pressure at 30,
40, and 50 percent chord and with thickness ratios varying from
6 percent to 15 percent. Also presented are data for a mean line
designed to maintain straight sides on the cambered sections.

The experimental results of a two-dimensional wind-tunnel
investigation of the aerodynamic characteristics of five NACA 64A-series
airfoil sections and two NACA 63A-series airfoil sections are
presented. An analysis of these results, which were obtained at
Reynolds numbers of 3×10^6, 6×10^6, and 9×10^6, indicates that
the section minimum-drag and maximum-lift characteristics of
comparable NACA 6-series and 6A-series airfoil sections are essen-
tially the same. The quarter-chord pitching-moment coefficients
and angles of zero lift of NACA 6A-series airfoil sections are
slightly more negative than those of corresponding NACA 6-series
airfoil sections. The position of the aerodynamic center and the
lift-curve slope of smooth NACA 6A-series airfoil sections appear
to be essentially independent of airfoil thickness ratio in contrast
to the trends shown by NACA 6-series sections. The addition of
standard leading-edge roughness causes the lift-curve slope of
the newer sections to decrease with increasing airfoil thickness
ratio.

INTRODUCTION

Much interest is being shown in airfoil sections having small
thickness ratios because of their high critical Mach numbers. The
NACA 6-series airfoil sections of small thickness have relatively
high critical Mach numbers but have the disadvantage of being very

2 NACA TN No. 1368

thin near the trailing edge, particularly when the sections considered
have the position of minimum pressure well forward on the basic
thickness form. The thin trailing-edge portions lead to difficulties
in structural design and fabrication. In order to overcome these
difficulties, the trailing-edge cusp has been removed from a number
of NACA 6-series basic thickness forms and the sides of the airfoil
sections made straight from approximately 80 percent chord to the
trailing edge. These new sections are designated NACA 6A-series air-
foil sections. A special mean line, designated the $a = 0.8$ (modified)
mean line, has also been designed to maintain straight sides on the
cambered sections.

This paper presents theoretical pressure-distribution data
and ordinates for NACA 6A-series basic thickness forms covering a
range of thickness ratios extending from 6 to 15 percent and a
range of positions of minimum pressure extending from 30 percent
to 50 percent chord.

The aerodynamic characteristics of seven NACA 6A-series airfoil
sections as determined in the Langley two-dimensional low-turbulence
pressure tunnel are also presented. These data are analyzed and
compared with similar data for NACA 6-series airfoil sections of
comparable thickness and design lift coefficient.

COEFFICIENTS AND SYMBOLS

c_d section drag coefficient

$c_{d_{min}}$ minimum section drag coefficient

c_l section lift coefficient

c_{l_i} design section lift coefficient

$c_{l_{max}}$ maximum section lift coefficient

$c_{m_{a.c.}}$ section pitching-moment coefficient about aerodynamic center

$c_{m_{c/4}}$ section pitching-moment coefficient about quarter-chord point

α_0 section angle of attack

α_i section angle of attack corresponding to design lift
        coefficient

$\dfrac{dc_l}{d\alpha_o}$ section lift-curve slope

V free-stream velocity

v local velocity

Δv increment of local velocity

Δv_a increment of local velocity caused by additional type of load distribution

P_R resultant pressure coefficient; difference between local upper-surface and lower-surface pressure coefficients

R Reynolds number

c airfoil chord length

x distance along chord from leading edge

y distance perpendicular to chord

y_c mean-line ordinate

a mean-line designation; fraction of chord from leading edge over which design load is uniform

ψ airfoil design parameter (reference 1)

THEORETICAL CHARACTERISTICS OF AIRFOILS

Designation.- The system used for designating the new airfoil sections is the same as that employed for the NACA 6-series sections (reference 1) except that the capital letter "A" is substituted for the dash which appears between the digit denoting the position of minimum pressure and that denoting the ideal lift coefficient. For example, the NACA 64_1-212 becomes the NACA 64_1A212 when the cusp is removed from the trailing edge. In the absence of any further modification of the designation, the cambered airfoils are to be considered as having the $a = 0.8$ (modified) mean line.

Basic thickness forms.- The theoretical methods by which the basic thickness forms of the NACA 6-series family of airfoil sections were derived in order to have pressure distributions of a specified

type are described in reference 1. Removing the trailing-edge cusp
was accomplished by increasing the value of the airfoil design
parameter ψ (reference 1) corresponding to the rear portion of the
airfoil until the airfoil ordinates formed a straight line from
approximately 80 percent chord to the trailing edge. Once the final
form of the ψ curves was established, the new pressure distribu-
tions corresponding to the modified thickness forms were calculated
by the usual methods as described in reference 1.

A comparison of the theoretical pressure distributions of an
NACA 64_1-012 airfoil section and an NACA 64_1A012 airfoil section
(fig. 1) indicates that removing the trailing-edge cusp has little
effect upon the velocities around the section. A slight reduction
of the peak negative pressure and flatter pressure gradient over
the forward and rearward portions of the airfoil section seem to
be the principal effects. The theoretical calculations also
indicate the presence of a trailing-edge stagnation point caused
by the finite trailing-edge angle of the NACA 6A-series sections.
This stagnation point is, of course, never realized experimentally.

Ordinates and theoretical pressure-distribution data for
NACA 6A-series basic thickness forms having the position of
minimum pressure at 30, 40, and 50 percent chord are presented
in figures 2 to 16 for airfoil thickness ratios of 6, 8, 10, 12,
and 15 percent. If intermediate thickness ratios involving a
change in thickness of not more than 1 to 2 percent are desired,
the ordinates of the basic thickness forms may be scaled linearly
without seriously altering the gradients of the theoretical pressure
distribution.

Mean line.- In order that the addition of camber not change
the pressure-gradients over the basic thickness form, a mean line
should be used which causes uniform load to be carried from the
leading edge to a point at least as far back as the position of
minimum pressure on the basic thickness form. The usual practice
is to camber NACA 6-series airfoil sections with the $a = 1.0$ type
of mean line because this mean line appears to be best for high
maximum lift coefficients and, contrary to theoretical predictions,
does not cause excessive quarter-chord pitching-moment coefficients.

The $a = 1.0$ type mean line was not considered desirable,
however, for the NACA 6A-series basic thickness forms because the
surfaces of the cambered airfoil sections would be curved near
the trailing edge. The type of mean line best suited for maintaining
straight sides on these newer sections would be one that is perfectly
straight from 80 percent chord to the trailing edge. Such a camber

line could be obtained by modifying an a = 0.7 mean line. Con-
sideration of the effect of mean-line loading upon the maximum lift
coefficient indicated, however, that a mean line having a uniform
load distribution as far back along the chord as possible was
desirable. It was found that the a = 0.8 type mean line could be
made straight from approximately 85 percent chord to the trailing
edge without causing a sharp break in the mean line and with very
little curvature between the 80-percent and 85-percent chord. The
aerodynamic advantages of using this mean line in preference to one
having uniform load to 70 percent chord were considered to be more
important than the slight curvature existing in the modified
a = 0.8 mean line. For this reason, all cambered NACA 6A-series
airfoil sections have employed the a = 0.8 (modified) mean line.

The ordinates and load-distribution data corresponding to a
design lift coefficient of 1.0 are presented in figure 17 for the
a = 0.8 (modified) mean line. The ordinates of a mean line having
any arbitrary design lift coefficient may be obtained simply by
multiplying the ordinates presented by the desired design lift
coefficient.

Cambered airfoils.- The method used for cambering the basic
thickness distributions of figures 2 to 16 with the mean line of
figure 17 is described and discussed in references 1 and 2. It
consists essentially in laying out the ordinates of the basic
thickness forms normal to the mean line at corresponding stations.
A discussion of the method employed for combining the theoretical
pressure-distribution data, presented in figures 2 to 17 for the
mean-line and basic-thickness distribution, to give the approximate
theoretical pressure distribution about a cambered or symmetrical
airfoil section at any lift coefficient is given in reference 1.

APPARATUS AND TESTS

Wind tunnel.- All the tests described herein were conducted
in the Langley two-dimensional low-turbulence pressure tunnel. The
test section of this tunnel measures 3 feet by 7.5 feet. The
models completely spanned the 3-foot dimension with the gaps
between the model and tunnel walls sealed to prevent air leakage.
Lift measurements were made by taking the difference between the
pressure reaction upon the floor and ceiling of the tunnel, drag
results were obtained by the wake-survey method, and pitching moments
were determined with a torque balance. A more complete description
of the tunnel and the method of obtaining and reducing the data
are contained in reference 1.

Models.- The seven airfoil sections for which the experimental aerodynamic characteristics were obtained are:

    NACA 63A010
    NACA 63A210

    NACA 64A010
    NACA 64A210, NACA 64_1A212, NACA 64_2A215
    NACA 64A410

The models representing the airfoil sections were of 24 inch chord and were constructed of laminated mahogany. The models were painted with lacquer and then sanded with No. 400 carborundum paper until aerodynamically smooth surfaces were obtained. The ordinates of the models tested are presented in table I.

Tests.- The tests of each smooth airfoil section consisted in measurements of the lift, drag, and quarter-chord pitching-moment coefficients at Reynolds numbers of 3×10^6, 6×10^6, and 9×10^6. In addition, the lift and drag characteristics of each section were determined at a Reynolds number of 6×10^6 with standard roughness applied to the leading edge of the model. The standard roughness employed on these 24-inch-chord models consisted of 0.011-inch-diameter carborundum grains spread over a surface length of 8 percent of the chord back from the leading edge on the upper and lower surfaces. The grains were thinly spread to cover from 5 to 10 percent of this area. In an effort to obtain some idea of the effectiveness of the airfoil sections when equipped with trailing-edge high-lift devices, each section was fitted with a simulated split flap deflected 60°. Lift measurements with the split flap were made at a Reynolds number of 6×10^6 with the airfoil leading edge both smooth and rough.

RESULTS

The results obtained from tests of the seven airfoil sections are presented in figures 18 to 24 in the form of standard aerodynamic coefficients representing the lift, drag, and quarter-chord pitching-moment characteristics of the airfoil sections. The calculated position of the aerodynamic center and the variation of the pitching-moment coefficient with lift coefficient about this point are also included in these data. The influence of the tunnel boundaries has

been removed from all the aerodynamic data by means of the following
equations (developed in reference 1):

$$c_d = 0.990c_d{}'$$

$$c_l = 0.973c_l{}'$$

$$c_{m_c/4} = 0.951c_{m_c/4}{}'$$

$$\alpha_o = 1.015\alpha_o{}'$$

where the primed quantities denote the measured coefficients.

DISCUSSION

Although the amount of systematic aerodynamic data presented
for NACA 6A-series airfoil sections is not large, it is enough to
indicate the relative merits of the NACA 6A-series airfoil sections
as compared with the NACA 6-series sections. The variation of the
important aerodynamic characteristics of the five NACA 64A-series
airfoils with the pertinent geometrical parameters of the airfoils
is shown in figures 25 to 31, together with comparable data for
NACA 64-series airfoils. The curves shown in figures 25 to 31 are
for the NACA 64-series airfoil sections and are taken from the
faired data of reference 1. The experimental points which appear
on these figures represent the results obtained for the NACA 64A-series
airfoil sections in the present investigation. Since only two
NACA 63A-series sections were tested, comparative results are not
presented for them. The effect of removing the cusp from the
NACA 63-series sections is about the same as that of removing the
cusp from the NACA 64-series sections.

The comparative data showing the effects upon the aerodynamic
characteristics of removing the trailing-edge cusp from NACA 6-series
airfoil sections should be used with caution if the cusp removal is
affected in some manner other than that indicated earlier in this
paper. For example, if the cusp should be removed from a cambered
airfoil by means of a straight-line fairing of the airfoil surfaces,
the amount of camber would be decreased near the trailing edge.
Naturally, the effect upon the aerodynamic characteristics of
removing the cusp in such a manner would not be the same as indicated
by the comparative results presented for NACA 6-series and 6A-series
airfoils.

Drag.- The variation of section minimum drag coefficient with airfoil thickness ratio at a Reynolds number of 6×10^6 is shown in figure 25 for NACA 64-series and NACA 64A-series airfoil sections of various cambers, both smooth and with standard leading-edge roughness. As with the NACA 64-series sections (reference 1), the minimum drag coefficients of the NACA 64A-series sections show no consistent variation with camber. Comparison of the data of figure 25 indicates that removing the cusp from the trailing edge has no appreciable effect upon the minimum drag coefficients of the airfoils, either smooth or with standard leading-edge roughness.

Increasing the Reynolds number from 3×10^6 to 9×10^6 has about the same effect upon the minimum drag coefficient of NACA 64A-series airfoils (figs. 18 to 24) as that indicated in reference 1 for the NACA 64-series airfoils.

Some differences exist in the drag coefficients of NACA 64- and 64A-series airfoils outside the low-drag range of lift coefficients but these differences are small and do not show any consistent trends (figs. 18 to 24 and reference 1).

Lift.- The section angle of zero lift as a function of thickness ratio is shown in figure 26 for NACA 64- and 64A-series airfoil sections of various cambers. These results show that the angle of zero lift is nearly independent of thickness and is primarily dependent upon the amount of camber for a particular type of mean line. Theoretical calculations made by use of the mean line data of figure 17 and reference 1 indicate that airfoils with the $a = 0.8$ (modified) mean line should have angles of zero lift less negative than those with the $a = 1.0$ mean line. Actually, the reverse appears to be the case, and this effect is due mainly to the fact that airfoils having the $a = 1.0$ type of mean line have angles of zero lift which are only about 74 percent of their theoretical value (reference 1), and those having the $a = 0.8$ (modified) mean lines have angles of zero lift larger than indicated by theory.

The measured lift-curve slopes corresponding to the NACA 64-series and NACA 64A-series airfoils of various cambers are presented in figure 27 as a function of airfoil thickness ratio. No consistent variation of lift-curve slope with camber or Reynolds number is shown by either type of airfoil. An increase in trailing-edge angle produced by removal of the cusp tends to reduce the lift-curve slope by an amount which increases with airfoil thickness (see references 3 and 4), but it appears that, for the 6A-series airfoils, this decrease in lift-curve slope is just enough to equal the normal increase caused by airfoil thickness because the present data for the

6A-sections show essentially no variation in lift-curve slope with thickness. The value of the lift-curve slope for smooth NACA 64A-series airfoil sections is very close to that predicted from thin airfoil theory (2π per radian or 0.110 per degree). Removing the trailing-edge cusp from an airfoil section with standard leading-edge roughness causes the lift-curve slope to decrease quite rapidly with increasing airfoil thickness ratio.

The variation of the maximum section lift coefficient with airfoil thickness ratio and camber at a Reynolds number of 6×10^6 is shown in figure 28 for NACA 64-series and NACA 64A-series airfoil sections with and without standard leading-edge roughness and simulated split flaps deflected $60°$. A comparison of these data indicates that the character of the variation of maximum lift coefficient with airfoil thickness ratio and camber is nearly the same for the NACA 64-series and NACA 64A-series airfoil sections. The magnitude of the maximum lift coefficient appears to be slightly less for the plain NACA 64A-series airfoils and slightly higher for the NACA 64A-series airfoils with split flaps than corresponding values for the NACA 64-series airfoils. These differences are small, however, and for engineering applications the maximum-lift characteristics of NACA 64-series and 64A-series airfoil sections of comparable thickness and design lift coefficient may be considered practically the same.

A comparison of the maximum-lift data for NACA 64A-series airfoil sections with similar data for NACA 64-series airfoil sections, presented in figures 18 to 24, indicates that the scale-effect characteristics of the two types of section are essentially the same for the range of Reynolds number from 3×10^6 to 9×10^6.

Pitching moment.- Thin-airfoil theory provides a means for calculating the theoretical quarter-chord pitching-moment coefficients of airfoil sections having various amounts and types of camber. Calculations were made according to these methods for airfoils having the $a = 1.0$ and $a = 0.8$ (modified) mean lines by using the theoretical mean-line data presented in figure 17 and in reference 1. The results of these calculations indicate that the quarter-chord pitching-moment coefficients of the NACA 64A-series airfoil sections having the $a = 0.8$ (modified) mean line should be only about 37 percent of those for the NACA 64-series airfoil sections with the $a = 1.0$ mean line. The experimental relationship between the quarter-chord pitching-moment coefficient and airfoil thickness ratio and camber, shown in figure 29, discloses that the plain NACA 64A-series airfoils have pitching-moment coefficients which are slightly more negative than those for the plain NACA 64-series airfoils. The increase in the magnitude of the

pitching-moment coefficient of NACA 64A-series airfoils as compared
with NACA 64-series airfoils becomes greater when the airfoils are
equipped with simulated split flaps deflected 60°. A comparison of
the theoretical and measured pitching-moment coefficients is shown
in figure 30 for NACA 64-series and 64A-series airfoil sections.
These comparative data indicate that the NACA 64A-series sections
much more nearly realize their theoretical moment coefficients
than do the 64-series airfoil sections. Similar trends have been
shown to result when mean lines such as the a = 0.5 type are
employed with NACA 6-series airfoils (reference 1).

Aerodynamic center.- The position of the aerodynamic center and
the variation of the moment coefficient with lift coefficient about
this point were calculated from the quarter-chord pitching-moment
data for each of the seven airfoils tested. The variation of the
chordwise position of the aerodynamic center with airfoil thickness
ratio is shown in figure 31 for the NACA 64-series and 64A-series
airfoil sections. Since the data for the NACA 64-series airfoils
showed no consistent variation with camber, the results are repre-
sented by a single faired curve for all cambers. Following this
same trend, the position of the aerodynamic center for the
NACA 64A-series airfoils shows no consistent variation with camber.
The data of figures 18 to 24 show that the variations in the Reynolds
number have no consistent effect upon the chordwise position of the
aerodynamic center.

Perfect fluid theory indicates that the position of the aero-
dynamic center should move rearward with increasing airfoil thickness
and the experimental results for the NACA 64-series airfoil sections
follow this trend. The data of reference 5 show important forward
movements of the aerodynamic center with increasing trailing-edge
angle for a given airfoil thickness ratio. The results obtained
for the NACA 24-, 44-, and 230-series airfoil sections (reference 1)
reveal that the effect of increasing trailing-edge angle predominates
over the effect of increasing thickness because the position of the
aerodynamic center moves forward with increasing thickness ratio
for these airfoil sections. For the NACA 64A-series airfoils
(fig. 31) the aerodynamic center is slightly behind the quarter-
chord point and does not appear to vary with increasing thickness.
These results suggest that the effect of increasing thickness is
counterbalanced by increasing trailing-edge angle for these airfoil
sections.

CONCLUSIONS

From a two-dimensional wind-tunnel investigation of the aero-dynamic characteristics of five NACA 64A-series and two NACA 63A-series airfoil sections the following conclusions based upon data obtained at Reynolds numbers of 3×10^6, 6×10^6, and 9×10^6 may be drawn:

1. The section minimum drag and maximum lift coefficients of corresponding NACA 6-series and 6A-series airfoil sections are essentially the same.

2. The lift-curve slopes of smooth NACA 6A-series airfoil sections appear to be essentially independent of airfoil thickness ratio, in contrast to the trends shown by NACA 6-series airfoil sections. The addition of standard leading-edge roughness causes the lift-curve slope to decrease with increasing airfoil thickness ratio for NACA 6A-series airfoil sections.

3. The section angles of zero lift of NACA 6A-series airfoil sections are slightly more negative than those of comparable NACA 6-series airfoil sections.

4. The section quarter-chord pitching-moment coefficients of NACA 6A-series airfoil sections are slightly more negative than those of comparable NACA 6-series airfoil sections. The position of the aerodynamic center is essentially independent of airfoil thickness ratio for NACA 6A-series airfoil sections.

Langley Memorial Aeronautical Laboratory
    National Advisory Committee for Aeronautics
        Langley Field, Va., May 6, 1947

REFERENCES

1. Abbott, Ira H., von Doenhoff, Albert E., and Stivers, Louis S., Jr.: Summary of Airfoil Data. NACA ACR No. L5C05, 1945.

2. Jacobs, Eastman N., Ward, Kenneth E., and Pinkerton, Robert M.: The Characteristics of 78 Related Airfoil Sections from Tests in the Variable-Density Wind Tunnel. NACA Rep. No. 460, 1933.

3. Purser, Paul E., and McKee, John W.: Wind-Tunnel Investigation of a Plain Aileron with Thickened and Beveled Trailing Edges on a Tapered Low-Drag Wing. NACA ACR, Jan. 1943.

4. Jones, Robert T., and Ames, Milton B., Jr.: Wind-Tunnel Investigation of Control-Surface Characteristics. V - The Use of a Beveled Trailing Edge to Reduce the Hinge Moment of a Control Surface. NACA ARR, March 1942.

5. Purser, Paul E., and Johnson, Harold S.: Effects of Trailing-Edge Modifications on Pitching-Moment Characteristics of Airfoils. NACA CB No. L4I30, 1944.

TABLE I

ORDINATES OF NACA 6A-SERIES AIRFOIL SECTION

NACA 63A010

[Stations and ordinates given in percent of airfoil chord]

Upper Surface		Lower Surface	
Station	Ordinate	Station	Ordinate
0	0	0	0
.5	.816	.5	-.816
.75	.983	.75	-.983
1.25	1.250	1.25	-1.250
2.5	1.737	2.5	-1.737
5.0	2.412	5.0	-2.412
7.5	2.917	7.5	-2.917
10	3.324	10	-3.324
15	3.950	15	-3.950
20	4.400	20	-4.400
25	4.714	25	-4.714
30	4.913	30	-4.913
35	4.995	35	-4.995
40	4.968	40	-4.968
45	4.837	45	-4.837
50	4.613	50	-4.613
55	4.311	55	-4.311
60	3.943	60	-3.943
65	3.517	65	-3.517
70	3.044	70	-3.044
75	2.545	75	-2.545
80	2.040	80	-2.040
85	1.535	85	-1.535
90	1.030	90	-1.030
95	.525	95	-.525
100	.021	100	-.021

L.E. radius: 0.742
T.E. radius: 0.023

NACA 63A210

[Stations and ordinates given in percent of airfoil chord]

Upper Surface		Lower Surface	
Station	Ordinate	Station	Ordinate
0	0	0	0
.423	.868	.577	-.756
.664	1.058	.836	-.900
1.151	1.367	1.349	-1.125
2.384	1.944	2.616	-1.522
4.869	2.769	5.131	-2.047
7.364	3.400	7.636	-2.428
9.863	3.917	10.137	-2.725
14.869	4.729	15.131	-3.167
19.882	5.328	20.118	-3.468
24.898	5.764	25.102	-3.662
29.916	6.060	30.084	-3.764
34.935	6.219	35.065	-3.771
39.955	6.247	40.045	-3.689
44.975	6.151	45.025	-3.523
49.994	5.943	50.006	-3.283
55.012	5.637	54.988	-2.985
60.028	5.245	59.972	-2.644
65.041	4.772	64.959	-2.262
70.052	4.227	69.948	-1.861
75.061	3.624	74.939	-1.464
80.074	2.974	79.926	-1.104
85.072	2.254	84.928	-.812
90.050	1.519	89.950	-.539
95.026	.769	94.974	-.279
100.000	.021	100.000	-.021

L.E. radius: 0.742
T.E. radius: 0.023
Slope of radius through L.E.: 0.095

NACA 64A010

[Stations and ordinates given in percent of airfoil chord]

Upper Surface		Lower Surface	
Station	Ordinate	Station	Ordinate
0	0	0	0
.5	.804	.5	-.804
.75	.969	.75	-.969
1.25	1.225	1.25	-1.225
2.5	1.688	2.5	-1.688
5.0	2.327	5.0	-2.327
7.5	2.805	7.5	-2.805
10	3.199	10	-3.199
15	3.813	15	-3.813
20	4.272	20	-4.272
25	4.606	25	-4.606
30	4.837	30	-4.837
35	4.968	35	-4.968
40	4.995	40	-4.995
45	4.894	45	-4.894
50	4.684	50	-4.684
55	4.388	55	-4.388
60	4.021	60	-4.021
65	3.597	65	-3.597
70	3.127	70	-3.127
75	2.623	75	-2.623
80	2.103	80	-2.103
85	1.582	85	-1.582
90	1.062	90	-1.062
95	.541	95	-.541
100	.021	100	-.021

L.E. radius: 0.687
T.E. radius: 0.023

NACA 64A210

[Stations and ordinates given in percent of airfoil chord]

Upper Surface		Lower Surface	
Station	Ordinate	Station	Ordinate
0	0	0	0
.424	.856	.576	-.744
.665	1.044	.835	-.886
1.155	1.342	1.347	-1.100
2.387	1.895	2.613	-1.473
4.874	2.685	5.126	-1.963
7.369	3.288	7.631	-2.316
9.868	3.792	10.132	-2.600
14.874	4.592	15.126	-3.030
19.885	5.200	20.115	-3.340
24.900	5.656	25.100	-3.554
29.917	5.984	30.083	-3.688
34.935	6.192	35.065	-3.744
39.955	6.274	40.045	-3.716
44.975	6.208	45.025	-3.580
49.994	6.014	50.006	-3.354
55.012	5.714	54.988	-3.062
60.028	5.323	59.972	-2.719
65.042	4.852	64.958	-2.342
70.054	4.310	69.946	-1.944
75.063	3.702	74.937	-1.582
80.076	3.037	79.924	-1.167
85.074	2.301	84.926	-.859
90.052	1.551	89.918	-.571
95.027	.785	94.974	-.495
100.000	.021	100.000	-.021

L.E. radius: 0.687
T.E. radius: 0.023
Slope of radius through L.E.: 0.095

NATIONAL ADVISORY
COMMITTEE FOR AERONAUTICS

TABLE I

ORDINATES OF NACA 6A-SERIES AIRFOIL SECTION -

Concluded

NACA 64A410

[Stations and ordinates given in
percent of airfoil chord]

Upper Surface		Lower Surface	
Station	Ordinate	Station	Ordinate
0	0	0	0
.350	.902	.650	-.678
.582	1.112	.918	-.796
1.059	1.451	1.441	-.969
2.276	2.095	2.724	-1.251
4.749	3.034	5.251	-1.592
7.230	3.865	7.770	-1.919
9.737	4.380	10.263	-1.996
14.748	5.366	15.252	-2.244
19.770	6.126	20.230	-2.406
24.800	6.705	25.200	-2.499
29.834	7.131	30.166	-2.557
34.871	7.414	35.129	-2.518
39.910	7.552	40.090	-2.436
44.950	7.522	45.050	-2.266
49.989	7.344	50.011	-2.024
55.025	7.040	54.975	-1.736
60.057	6.624	59.943	-1.418
65.085	6.106	64.915	-1.086
70.108	5.490	69.892	-.760
75.126	4.780	74.874	-.460
80.151	3.967	79.849	-.229
85.148	3.018	84.852	-.132
90.104	2.038	89.896	-.076
95.053	1.028	94.947	-.048
100.000	.021	100.000	-.021

L.E. radius: 0.687
T.E. radius: 0.023
Slope of radius through L.E.: 0.190

NACA 64₁A212

[Stations and ordinates given in
percent of airfoil chord]

Upper Surface		Lower Surface	
Station	Ordinate	Station	Ordinate
0	0	0	0
.409	1.013	.591	-.901
.648	1.233	.852	-1.075
1.135	1.580	1.365	-1.338
2.365	2.225	2.635	-1.803
4.849	3.145	5.151	-2.423
7.343	3.846	7.657	-2.874
9.842	4.432	10.158	-3.240
14.849	5.358	15.151	-3.796
19.862	6.080	20.138	-4.200
24.880	6.584	25.120	-4.482
29.900	6.956	30.100	-4.660
34.922	7.189	35.078	-4.741
39.946	7.272	40.054	-4.714
44.970	7.177	45.030	-4.549
49.993	6.935	50.007	-4.275
55.015	6.570	54.985	-3.918
60.034	6.103	59.966	-3.499
65.050	5.544	64.950	-3.034
70.064	4.903	69.936	-2.537
75.075	4.197	74.925	-2.037
80.090	3.433	79.910	-1.563
85.088	2.601	84.912	-1.159
90.062	1.751	89.938	-.771
95.032	.888	94.968	-.598
100.000	.025	100.000	-.025

L.E. radius: 0.994
T.E. radius: 0.028
Slope of radius through L.E.: 0.095

NACA 64₂A215

[Stations and ordinates given in
percent of airfoil chord]

Upper Surface		Lower Surface	
Station	Ordinate	Station	Ordinate
0	0	0	0
.388	1.243	.612	-1.131
.624	1.509	.876	-1.351
1.107	1.930	1.393	-1.688
2.333	2.713	2.667	-2.291
4.811	3.833	5.189	-3.111
7.304	4.685	7.696	-3.711
9.802	5.391	10.198	-4.199
14.811	6.510	15.189	-4.948
19.827	7.351	20.173	-5.491
24.849	7.975	25.151	-5.873
29.875	8.417	30.125	-6.121
34.903	8.686	35.097	-6.238
39.933	8.766	40.067	-6.208
44.963	8.627	45.037	-5.999
49.992	8.308	50.008	-5.648
55.018	7.843	54.982	-5.191
60.042	7.258	59.958	-4.654
65.063	6.566	64.937	-4.056
70.079	5.782	69.921	-3.416
75.093	4.926	74.907	-2.766
80.111	4.017	79.889	-2.147
85.109	3.039	84.891	-1.597
90.076	2.046	89.924	-1.066
95.039	1.039	94.961	-.549
100.000	.032	100.000	-.032

L.E. radius: 1.561
T.E. radius: 0.037
Slope of radius through L.E.: 0.095
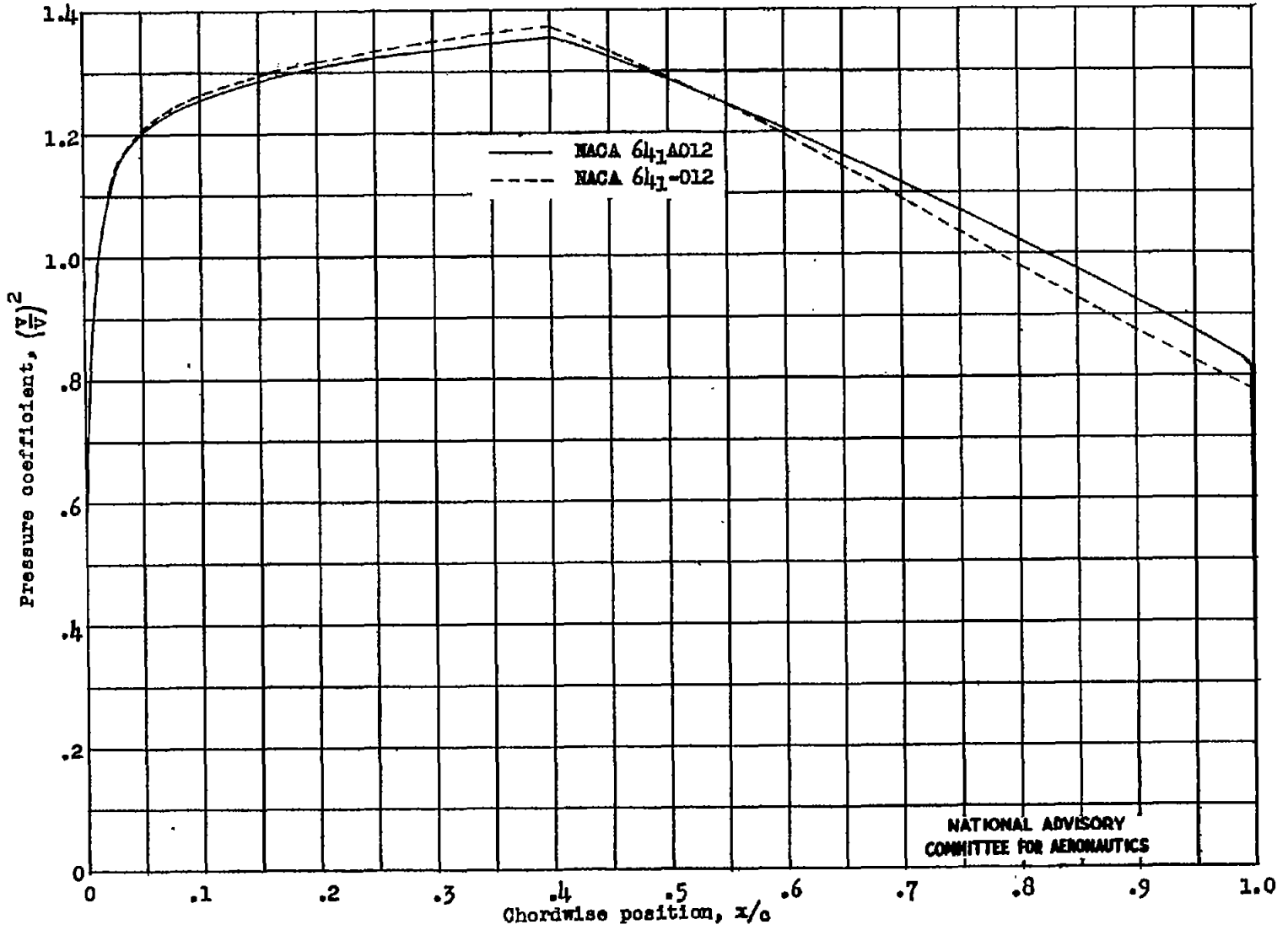
Figure 1.- Comparison of theoretical pressure distribution at zero
lift of the NACA 64_1-012 and the NACA 64_1A012 airfoil sections.

Fig. 1

Fig. 2   NACA TN No. 1368
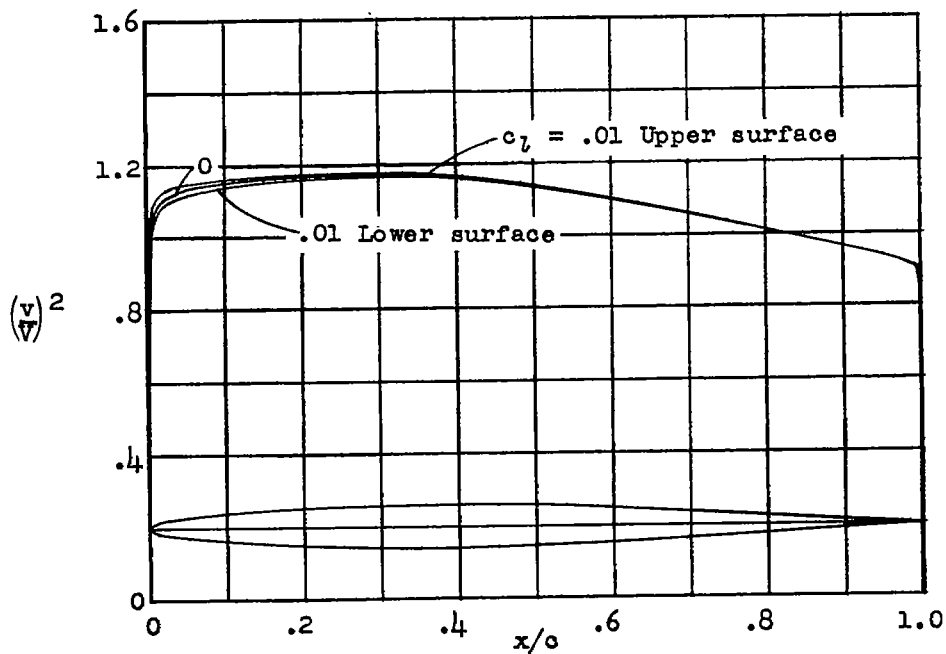
x (percent c)	y (percent c)	$(v/V)^2$	v/V	$\Delta v_a/V$
0	0	0	0	4.560
.5	.495	.900	.949	2.079
.75	.595	1.063	1.031	1.794
1.25	.754	1.086	1.042	1.370
2.5	1.045	1.112	1.055	.976
5.0	1.447	1.134	1.065	.693
7.5	1.747	1.142	1.069	.563
10	1.989	1.150	1.072	.485
15	2.362	1.159	1.077	.383
20	2.631	1.165	1.079	.321
25	2.820	1.168	1.081	.278
30	2.942	1.170	1.082	.244
35	2.996	1.169	1.081	.217
40	2.985	1.162	1.078	.195
45	2.914	1.151	1.073	.175
50	2.788	1.138	1.067	.158
55	2.613	1.120	1.058	.140
60	2.396	1.100	1.049	.126
65	2.143	1.079	1.039	.112
70	1.859	1.057	1.028	.098
75	1.556	1.035	1.017	.085
80	1.248	1.010	1.005	.072
85	.939	.986	.993	.060
90	.630	.964	.982	.047
95	.322	.939	.969	.033
100	.013	0	0	0

L.E. radius: 0.265 percent c
T.E. radius: 0.014 percent c

Figure 2.- NACA 63A006 basic thickness form.
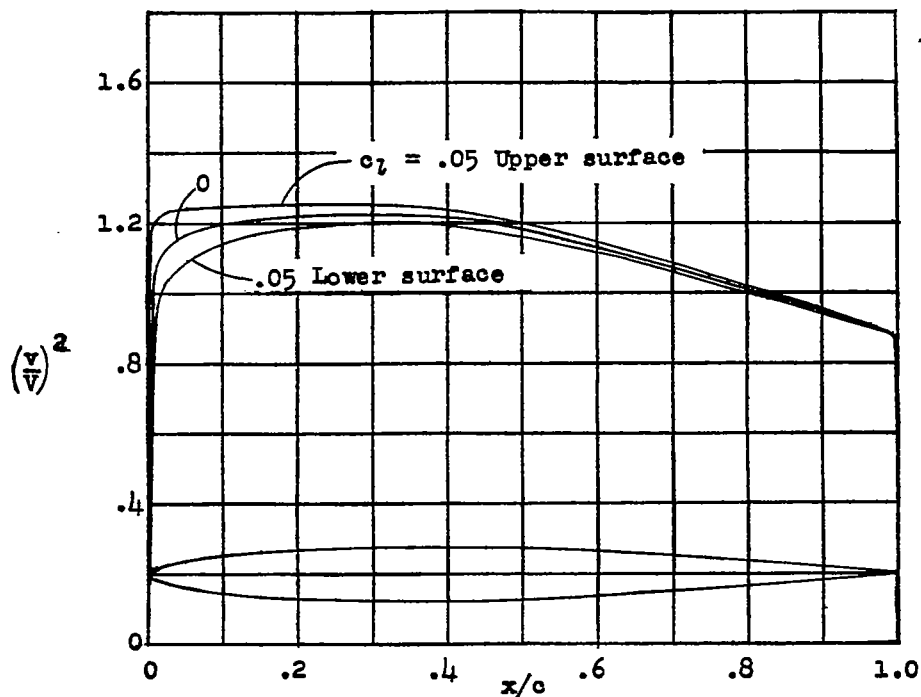
x (percent c)	y (percent c)	$(v/V)^2$	v/V	$\Delta v_a/V$
0	0	0	0	3.465
.5	.658	.850	.922	1.961
.75	.791	1.034	1.017	1.674
1.25	1.003	1.080	1.039	1.344
2.5	1.391	1.132	1.064	.967
5.0	1.930	1.168	1.081	.689
7.5	2.332	1.185	1.089	.562
10	2.656	1.198	1.095	.484
15	3.155	1.212	1.101	.383
20	3.515	1.221	1.105	.322
25	3.766	1.227	1.108	.279
30	3.926	1.230	1.109	.246
35	3.995	1.228	1.108	.218
40	3.978	1.219	1.104	.195
45	3.878	1.204	1.097	.174
50	3.705	1.183	1.088	.156
55	3.468	1.159	1.077	.138
60	3.176	1.132	1.064	.123
65	2.837	1.104	1.051	.109
70	2.457	1.073	1.036	.096
75	2.055	1.042	1.021	.083
80	1.647	1.010	1.005	.070
85	1.240	.980	.990	.058
90	.833	.951	.975	.045
95	.425	.919	.959	.030
100	.018	0	0	0

L.E. radius: 0.473 percent c
T.E. radius: 0.020 percent c

Figure 3.- NACA 63A008 basic thickness form.

Fig. 4   NACA TN No. 1368

Figure 4.- NACA 63A010 basic thickness form.
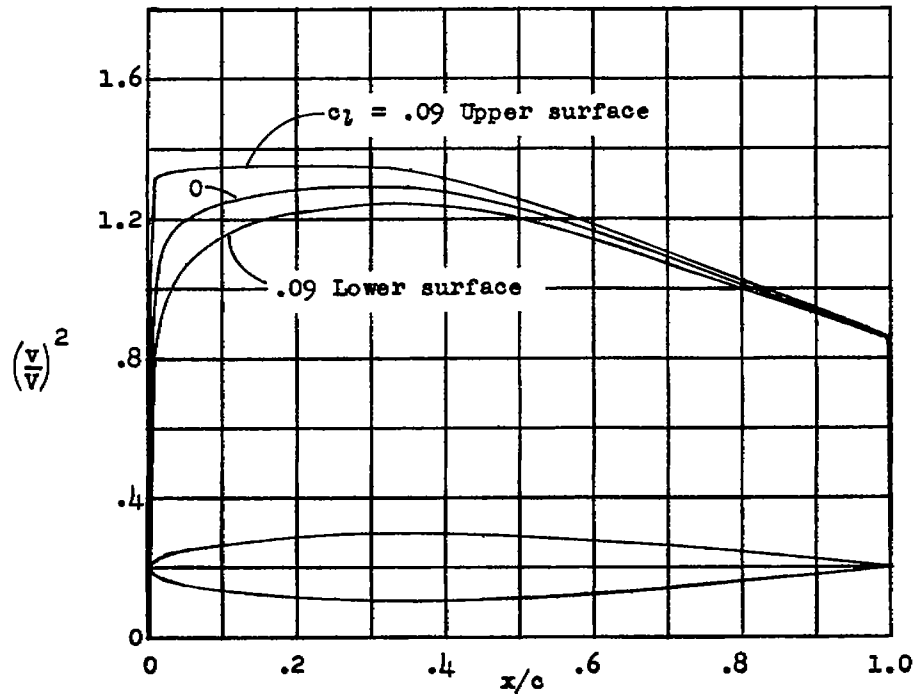
x (percent c)	y (percent c)	$(v/V)^2$	v/V	$\Delta v_a/V$
0	0	0	0	2.805
.5	.816	.774	.880	1.833
.75	.983	.985	.992	1.594
1.25	1.250	1.043	1.021	1.307
2.5	1.737	1.140	1.068	.957
5.0	2.412	1.200	1.095	.684
7.5	2.917	1.225	1.107	.560
10	3.324	1.245	1.116	.483
15	3.950	1.268	1.126	.383
20	4.400	1.282	1.132	.324
25	4.714	1.290	1.136	.280
30	4.913	1.294	1.138	.247
35	4.995	1.291	1.136	.218
40	4.968	1.279	1.131	.195
45	4.837	1.258	1.122	.174
50	4.613	1.230	1.109	.155
55	4.311	1.196	1.094	.137
60	3.943	1.162	1.078	.122
65	3.517	1.125	1.061	.108
70	3.044	1.086	1.042	.094
75	2.545	1.048	1.024	.081
80	2.040	1.009	1.004	.068
85	1.535	.972	.986	.057
90	1.030	.938	.969	.044
95	.525	.900	.949	.030
100	.021	0	0	0

L.E. radius: 0.742 percent c
T.E. radius: 0.023 percent c

Figure 4.- NACA 63A010 basic thickness form.

NATIONAL ADVISORY
COMMITTEE FOR AERONAUTICS
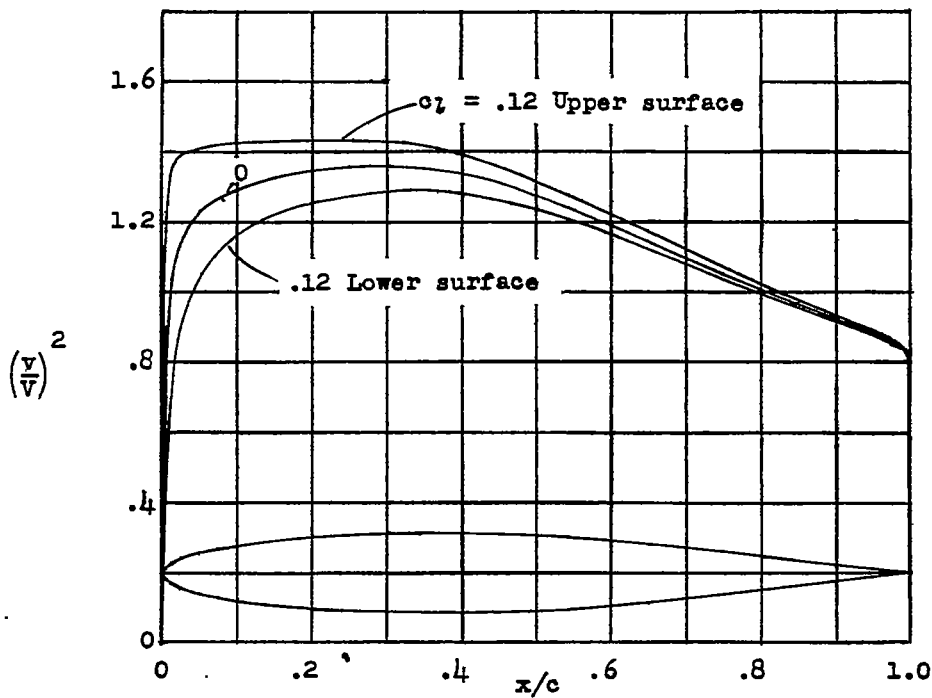
x (percent c)	y (percent c)	$(v/V)^2$	v/V	$\Delta v_a/V$
0	0	0	0	2.361
.5	.973	.686	.828	1.701
.75	1.173	.924	.961	1.515
1.25	1.492	.985	.992	1.258
2.5	2.078	1.136	1.066	.935
5.0	2.895	1.229	1.109	.679
7.5	3.504	1.265	1.125	.559
10	3.994	1.291	1.136	.482
15	4.747	1.324	1.151	.384
20	5.287	1.344	1.159	.325
25	5.664	1.355	1.164	.281
30	5.901	1.360	1.166	.248
35	5.995	1.357	1.165	.219
40	5.957	1.340	1.158	.196
45	5.792	1.312	1.145	.174
50	5.517	1.275	1.129	.154
55	5.148	1.234	1.111	.136
60	4.700	1.191	1.091	.120
65	4.186	1.145	1.070	.106
70	3.621	1.098	1.048	.092
75	3.026	1.051	1.025	.079
80	2.426	1.007	1.003	.066
85	1.826	.964	.982	.055
90	1.225	.925	.962	.042
95	.625	.880	.938	.029
100	.025	0	0	0

L.E. radius: 1.071 percent c
T.E. radius: 0.028 percent c

Figure 5.- NACA 63_1A012 basic thickness form.

Fig. 6   NACA TN No. 1368
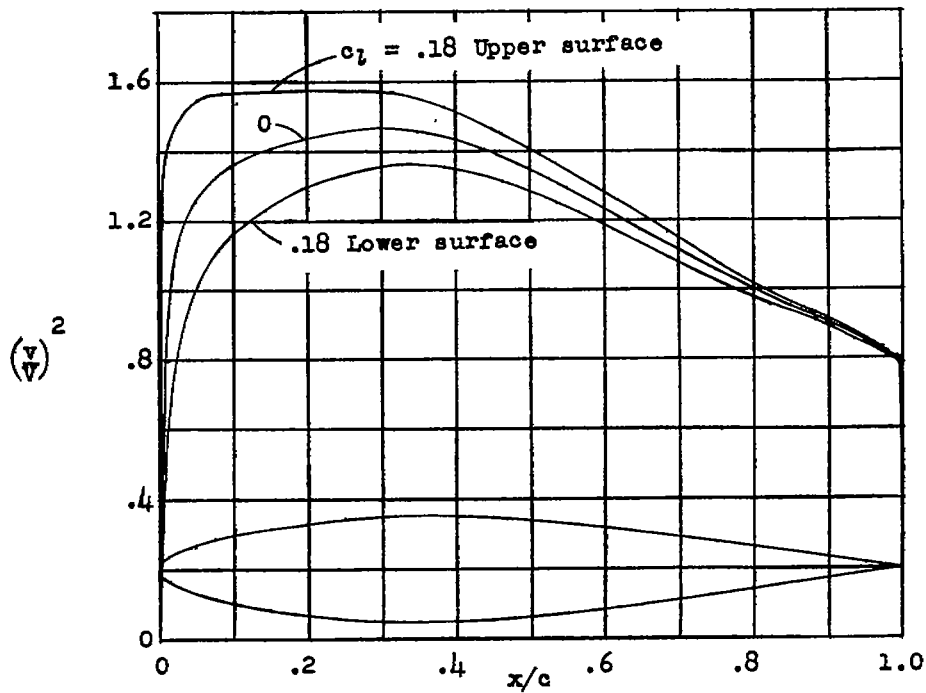
x (percent c)	y (percent c)	$(v/V)^2$	v/V	$\Delta v_a/V$
0	0	0	0	1.930
.5	1.203	.550	.742	1.504
.75	1.448	.825	.908	1.370
1.25	1.844	.882	.939	1.176
2.5	2.579	1.120	1.058	.905
5.0	3.618	1.257	1.121	.669
7.5	4.382	1.323	1.150	.555
10	4.997	1.361	1.167	.482
15	5.942	1.408	1.187	.384
20	6.619	1.437	1.199	.326
25	7.091	1.455	1.206	.282
30	7.384	1.464	1.210	.250
35	7.496	1.458	1.207	.220
40	7.435	1.435	1.198	.196
45	7.215	1.396	1.182	.174
50	6.858	1.349	1.161	.152
55	6.387	1.296	1.138	.134
60	5.820	1.237	1.112	.118
65	5.173	1.175	1.084	.104
70	4.468	1.115	1.056	.090
75	3.731	1.055	1.027	.077
80	2.991	1.000	1.000	.064
85	2.252	.950	.975	.052
90	1.512	.900	.949	.040
95	.772	.850	.922	.028
100	.032	0	0	0

L.E. radius: 1.630 percent c
T.E. radius: 0.037 percent c

Figure 6.- NACA 63_2A015 basic thickness form.
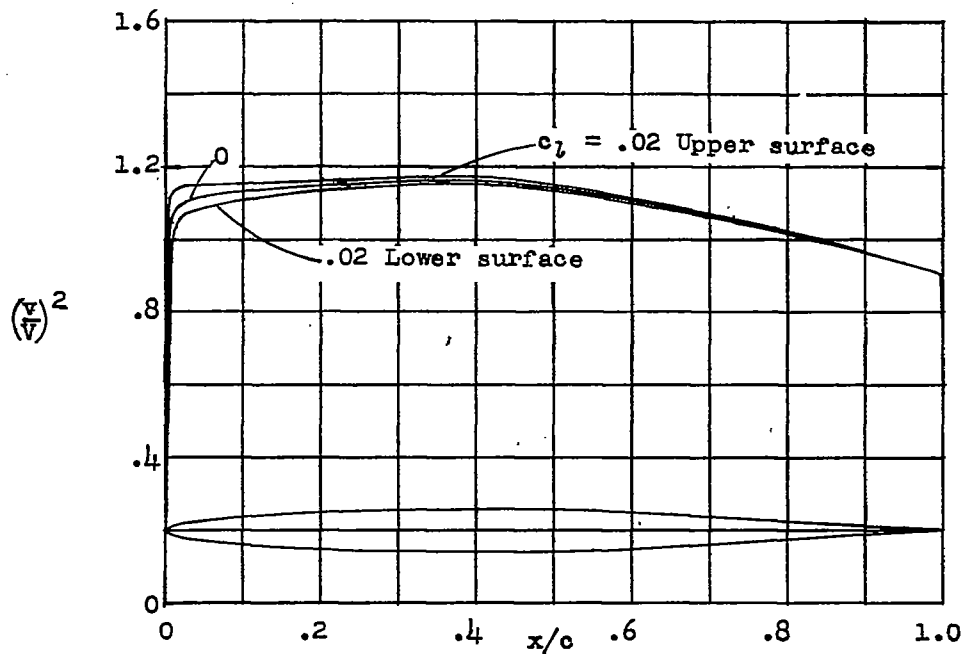
| x (percent c)	y (percent c)	$(v/V)^2$	v/V	$\Delta v_a/V$
0	0	0	0	4.688
.5	.485	1.019	1.009	2.101
.75	.585	1.046	1.023	1.798
1.25	.739	1.076	1.037	1.422
2.5	1.016	1.106	1.052	.980
5.0	1.399	1.118	1.057	.694
7.5	1.684	1.126	1.061	.564
10	1.919	1.132	1.064	.482
15	2.283	1.141	1.068	.382
20	2.557	1.149	1.072	.321
25	2.757	1.154	1.074	.278
30	2.896	1.158	1.076	.246
35	2.977	1.162	1.078	.219
40	2.999	1.165	1.079	.197
45	2.945	1.156	1.075	.177
50	2.825	1.142	1.069	.159
55	2.653	1.125	1.061	.143
60	2.438	1.107	1.052	.126
65	2.188	1.087	1.043	.112
70	1.907	1.066	1.032	.099
75	1.602	1.043	1.021	.087
80	1.285	1.018	1.009	.074
85	.967	.992	.996	.061
90	.649	.964	.982	.047
95	.331	.935	.967	.033
100	.013	0	0	0

L.E. radius: 0.246 percent c
T.E. radius: 0.014 percent c

Figure 7.- NACA 64A006 basic thickness form.

Fig. 8   NACA TN No. 1368
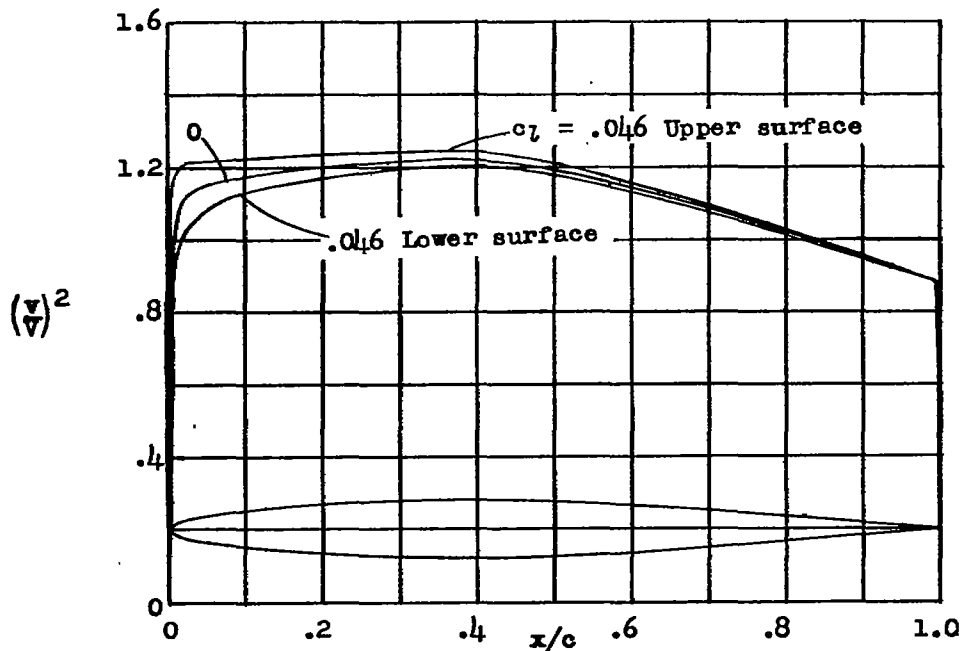
x (percent c)	y (percent c)	$(v/V)^2$	v/V	$\Delta v_a/V$
0	0	0	0	3.546
.5	.646	.947	.973	1.972
.75	.778	1.005	1.002	1.697
1.25	.983	1.068	1.033	1.352
2.5	1.353	1.122	1.059	.971
5.0	1.863	1.151	1.073	.692
7.5	2.245	1.165	1.079	.564
10	2.559	1.176	1.084	.481
15	3.047	1.191	1.091	.382
20	3.414	1.201	1.096	.323
25	3.681	1.209	1.100	.279
30	3.866	1.217	1.103	.247
35	3.972	1.221	1.105	.221
40	3.998	1.225	1.107	.198
45	3.921	1.211	1.100	.177
50	3.757	1.191	1.091	.158
55	3.524	1.167	1.080	.141
60	3.234	1.141	1.068	.125
65	2.897	1.113	1.055	.111
70	2.521	1.084	1.041	.098
75	2.117	1.053	1.026	.084
80	1.698	1.020	1.010	.072
85	1.278	.987	.993	.059
90	.858	.951	.975	.045
95	.438	.914	.956	.032
100	.018	0	0	0

L.E. radius: 0.439 percent c
T.E. radius: 0.020 percent c

Figure 8.- NACA 64A008 basic thickness form.
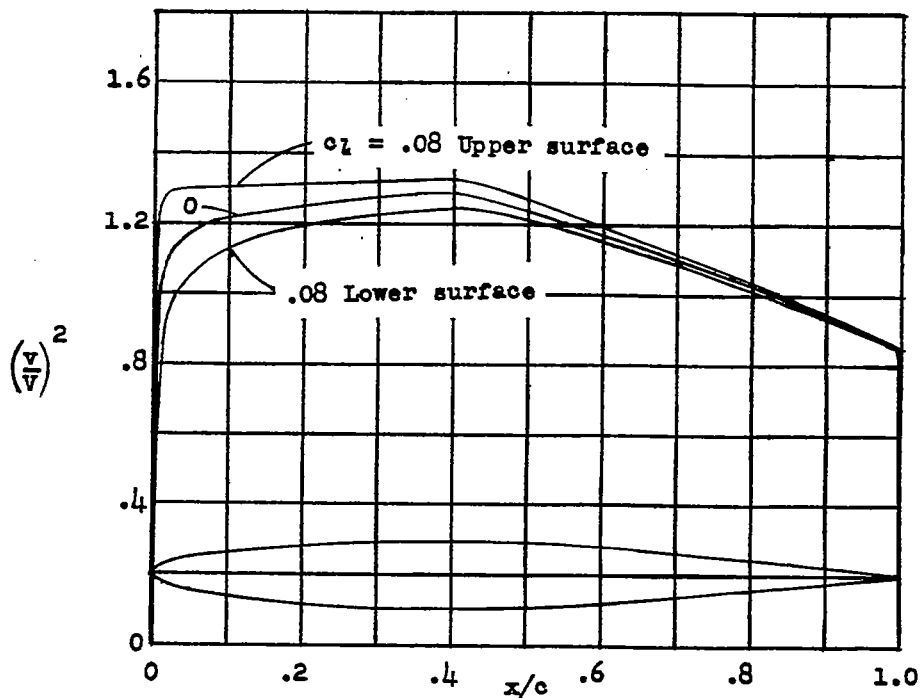
x (percent c)	y (percent c)	$(v/V)^2$	v/V	$\Delta v_a/V$
0	0	0	0	2.868
.5	.804	.868	.932	1.845
.75	.969	.952	.976	1.603
1.25	1.225	1.042	1.021	1.300
2.5	1.688	1.130	1.063	.957
5.0	2.327	1.178	1.085	.688
7.5	2.905	1.201	1.096	.562
10	3.199	1.217	1.103	.480
15	3.813	1.238	1.113	.382
20	4.272	1.254	1.120	.324
25	4.606	1.266	1.125	.280
30	4.837	1.275	1.129	.248
35	4.968	1.282	1.132	.221
40	4.995	1.288	1.135	.199
45	4.894	1.268	1.126	.177
50	4.684	1.240	1.114	.158
55	4.388	1.208	1.099	.140
60	4.021	1.174	1.084	.124
65	3.597	1.139	1.067	.109
70	3.127	1.102	1.050	.096
75	2.623	1.063	1.031	.083
80	2.103	1.023	1.011	.070
85	1.582	.981	.990	.058
90	1.062	.938	.969	.044
95	.541	.893	.945	.031
100	.021	0	0	0

L.E. radius: 0.687 percent c
T.E. radius: 0.023 percent c

Figure 9.- NACA 64A010 basic thickness form.

Fig. 10   NACA TN No. 1368
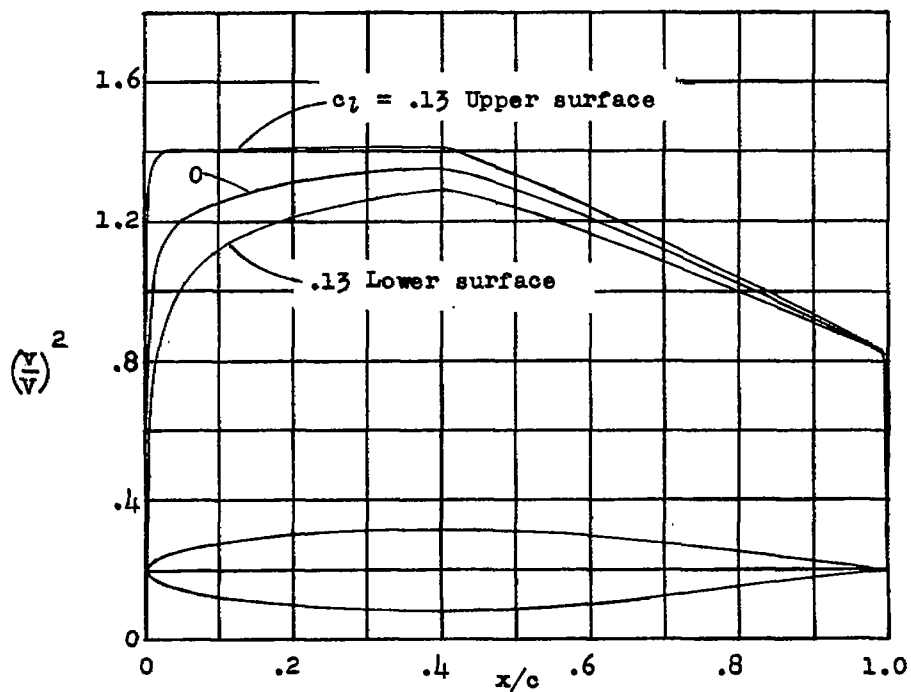
$\frac{x}{\text{(percent }c)}$	$\frac{y}{\text{(percent }c)}$	$(v/V)^2$	v/V	$\Delta v_a/V$
0	0	0	0	2.408
.5	.961	.792	.890	1.720
.75	1.158	.893	.945	1.515
1.25	1.464	1.006	1.003	1.254
2.5	2.018	1.127	1.062	.941
5.0	2.788	1.201	1.096	.681
7.5	3.364	1.235	1.111	.560
10	3.839	1.257	1.121	.478
15	4.580	1.288	1.135	.383
20	5.132	1.308	1.144	.325
25	5.534	1.324	1.151	.281
30	5.809	1.336	1.156	.249
35	5.965	1.346	1.160	.221
40	5.993	1.354	1.164	.199
45	5.863	1.326	1.152	.177
50	5.605	1.289	1.135	.157
55	5.244	1.250	1.118	.139
60	4.801	1.207	1.099	.123
65	4.289	1.164	1.079	.108
70	3.721	1.118	1.057	.094
75	3.118	1.071	1.035	.080
80	2.500	1.023	1.011	.068
85	1.882	.974	.987	.056
90	1.263	.925	.962	.042
95	.644	.873	.934	.029
100	.025	0	0	0

L.E. radius: 0.994 percent c
T.E. radius: 0.028 percent c

Figure 10.- NACA 64_1A012 basic thickness form.
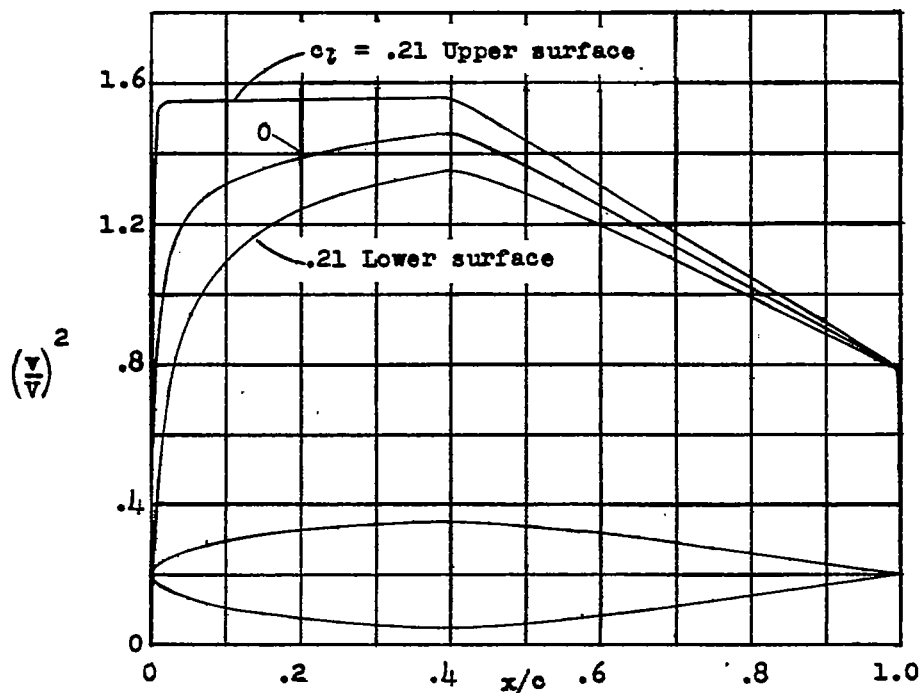
x (percent c)	y (percent c)	$(v/V)^2$	v/V	$\Delta v_a/V$
0	0	0	0	1.956
.5	1.193	.678	.823	1.552
.75	1.436	.789	.888	1.404
1.25	1.815	.936	.967	1.189
2.5	2.508	1.110	1.054	.912
5.0	3.477	1.226	1.107	.671
7.5	4.202	1.280	1.131	.552
10	4.799	1.314	1.146	.478
15	5.732	1.360	1.166	.384
20	6.423	1.390	1.179	.326
25	6.926	1.413	1.189	.283
30	7.270	1.430	1.196	.249
35	7.463	1.445	1.202	.222
40	7.487	1.458	1.207	.201
45	7.313	1.414	1.189	.177
50	6.978	1.364	1.168	.156
55	6.517	1.311	1.145	.137
60	5.956	1.255	1.120	.121
65	5.311	1.198	1.095	.106
70	4.600	1.139	1.067	.091
75	3.847	1.079	1.039	.078
80	3.084	1.020	1.010	.065
85	2.321	.961	.980	.053
90	1.558	.901	.949	.041
95	.795	.843	.918	.027
100	.032	0	0	0

L.E. radius: 1.561 percent c
T.E. radius: 0.037 percent c

Figure 11.- NACA 64_2A015 basic thickness form.

NATIONAL ADVISORY
COMMITTEE FOR AERONAUTICS

Fig. 12   NACA TN No. 1368

$$\left(\frac{v}{V}\right)^2$$

$c_l = .01$ Upper surface

.01 Lower surface

x/c
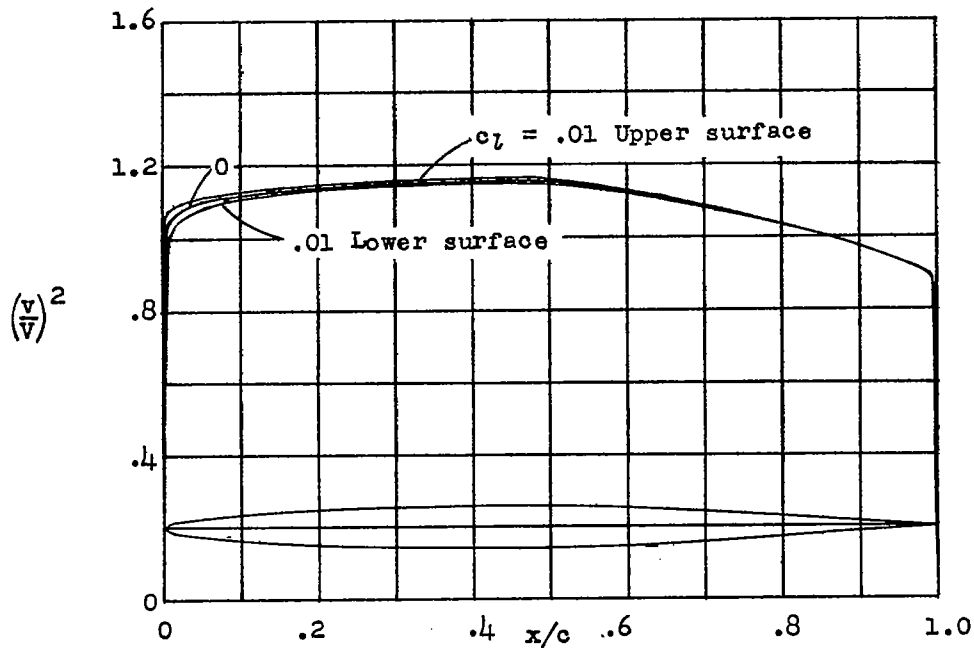
x (percent c)	y (percent c)	$(v/V)^2$	v/V	$\Delta v_a/V$
0	0	0	0	4.879
.5	.464	1.034	1.017	2.145
.75	.563	1.043	1.021	1.763
1.25	.718	1.058	1.029	1.365
2.5	.981	1.080	1.039	.966
5.0	1.313	1.101	1.049	.688
7.5	1.591	1.112	1.055	.562
10	1.824	1.120	1.058	.480
15	2.194	1.131	1.063	.382
20	2.474	1.139	1.067	.323
25	2.687	1.145	1.070	.278
30	2.842	1.149	1.072	.246
35	2.945	1.153	1.074	.219
40	2.996	1.157	1.076	.198
45	2.992	1.159	1.077	.178
50	2.925	1.157	1.076	.161
55	2.793	1.141	1.068	.143
60	2.602	1.124	1.060	.127
65	2.364	1.106	1.052	.112
70	2.087	1.083	1.041	.099
75	1.775	1.059	1.029	.087
80	1.437	1.032	1.016	.076
85	1.083	1.003	1.001	.061
90	.727	.973	.986	.047
95	.370	.936	.967	.033
100	.013	0	0	0

L.E. radius: 0.229 percent c
T.E. radius: 0.014 percent c

Figure 12.- NACA 65A006 basic thickness form.

NATIONAL ADVISORY
COMMITTEE FOR AERONAUTICS
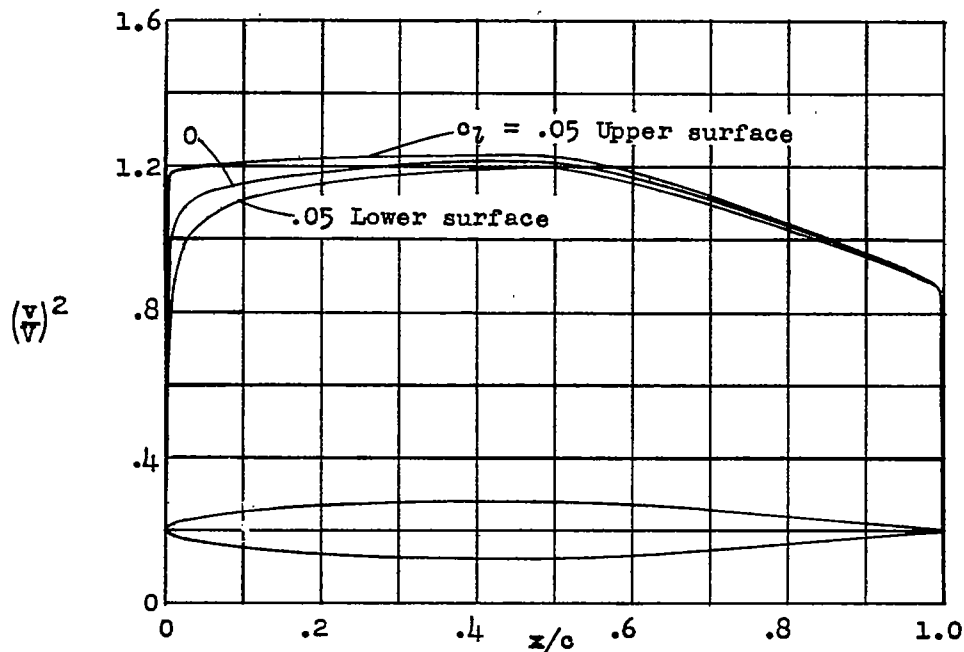
x (percent c)	y (percent c)	$(v/V)^2$	v/V	$\Delta v_a/V$
0	0	0	0	3.698
.5	.615	.973	.986	2.010
.75	.746	1.001	1.000	1.693
1.25	.951	1.038	1.019	1.333
2.5	1.303	1.088	1.043	.954
5.0	1.749	1.127	1.062	.685
7.5	2.120	1.145	1.070	.561
10	2.432	1.157	1.076	.479
15	2.926	1.175	1.084	.382
20	3.301	1.186	1.089	.322
25	3.585	1.195	1.093	.279
30	3.791	1.202	1.096	.247
35	3.928	1.207	1.099	.219
40	3.995	1.213	1.101	.198
45	3.988	1.217	1.103	.178
50	3.895	1.214	1.102	.161
55	3.714	1.191	1.091	.144
60	3.456	1.167	1.080	.128
65	3.135	1.139	1.067	.112
70	2.763	1.108	1.053	.098
75	2.348	1.076	1.037	.086
80	1.898	1.041	1.020	.073
85	1.430	1.002	1.001	.060
90	.960	.961	.980	.046
95	.489	.916	.957	.031
100	.018	0	0	0

L.E. radius: 0.408 percent c
T.E. radius: 0.020 percent c

Figure 13.- NACA 65A008 basic thickness form.

Fig. 14   NACA TN No. 1368
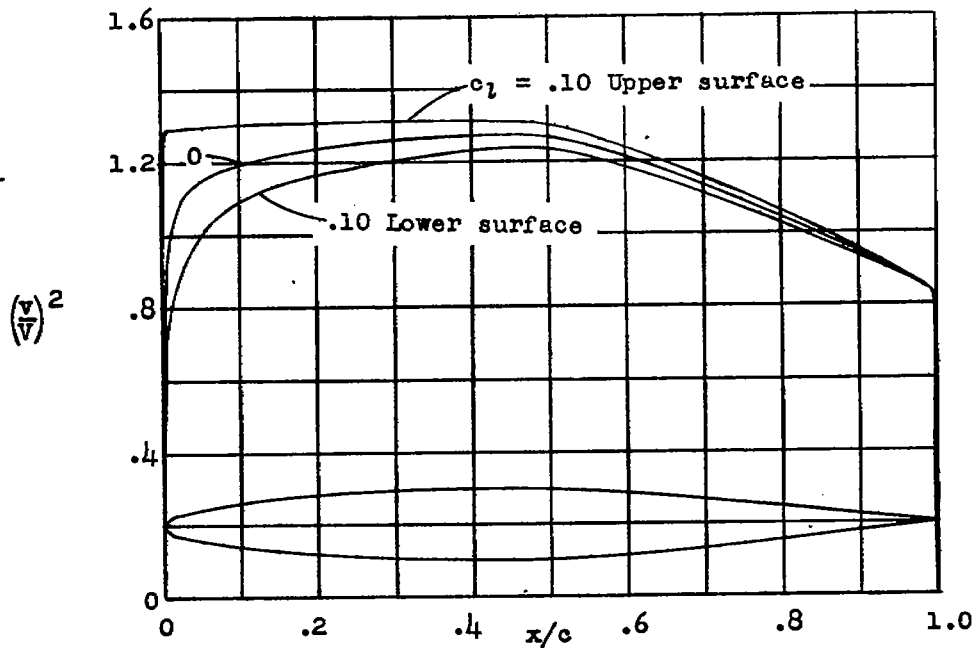
x (percent c)	y (percent c)	$(v/V)^2$	v/V	$\Delta v_a/V$
0	0	0	0	2.987
.5	.765	.897	.947	1.878
.75	.928	.948	.974	1.619
1.25	1.183	1.010	1.005	1.303
2.5	1.623	1.089	1.044	.936
5.0	2.182	1.148	1.071	.679
7.5	2.650	1.176	1.084	.559
10	3.040	1.194	1.093	.478
15	3.658	1.218	1.104	.382
20	4.127	1.234	1.111	.323
25	4.483	1.247	1.117	.281
30	4.742	1.257	1.121	.249
35	4.912	1.265	1.125	.222
40	4.995	1.272	1.128	.198
45	4.983	1.277	1.130	.178
50	4.863	1.271	1.127	.161
55	4.632	1.241	1.114	.144
60	4.304	1.208	1.099	.127
65	3.899	1.172	1.083	.111
70	3.432	1.133	1.064	.097
75	2.912	1.091	1.045	.084
80	2.352	1.047	1.023	.071
85	1.771	.999	.999	.058
90	1.188	.949	.974	.045
95	.604	.893	.945	.029
100	.021	0	0	0

L.E. radius: 0.639 percent c
T.E. radius: 0.023 percent c

Figure 14.- NACA 65A010 basic thickness form.
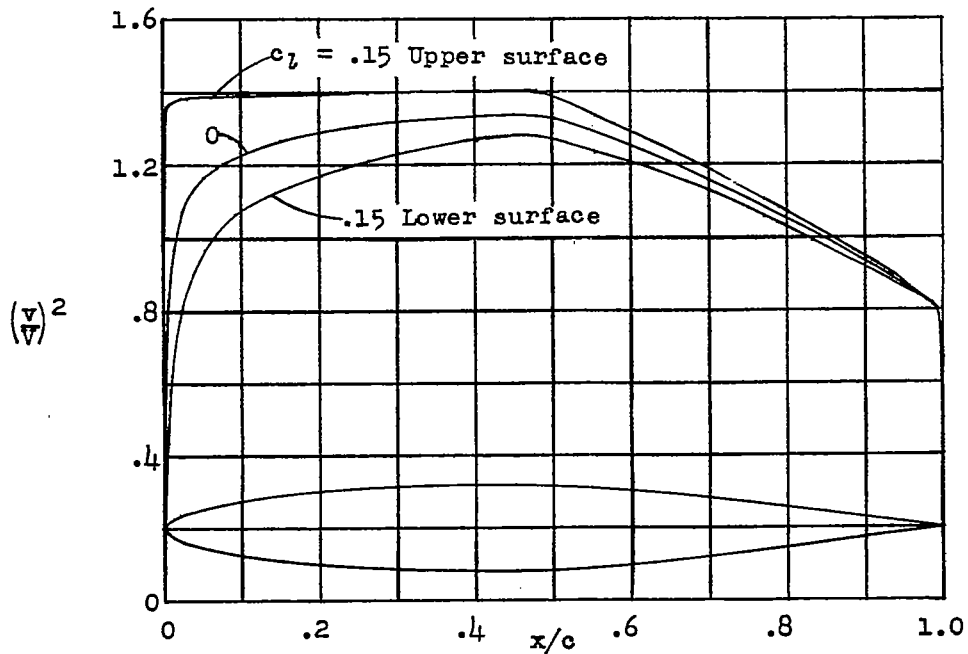
x (percent c)	y (percent c)	$(v/V)^2$	v/V	$\Delta v_a/V$
0	0	0	0	2.520
.5	.913	.824	.908	1.757
.75	1.106	.883	.940	1.543
1.25	1.414	.969	.984	1.263
2.5	1.942	1.081	1.040	.914
5.0	2.614	1.166	1.080	.672
7.5	3.176	1.204	1.097	.557
10	3.647	1.228	1.108	.477
15	4.392	1.263	1.124	.382
20	4.956	1.285	1.134	.324
25	5.383	1.301	1.141	.281
30	5.693	1.313	1.146	.250
35	5.897	1.324	1.151	.224
40	5.995	1.332	1.154	.198
45	5.977	1.338	1.157	.178
50	5.828	1.329	1.153	.161
55	5.544	1.292	1.137	.143
60	5.143	1.251	1.118	.126
65	4.654	1.204	1.097	.111
70	4.091	1.156	1.075	.096
75	3.467	1.104	1.051	.082
80	2.798	1.051	1.025	.069
85	2.106	.994	.997	.057
90	1.413	.936	.967	.043
95	.719	.871	.933	.027
100	.025	0	0	0

L.E. radius: 0.922 percent c
T.E. radius: 0.029 percent c

Figure 15.- NACA 65_1A012 basic thickness form.

Fig. 16   NACA TN No. 1368
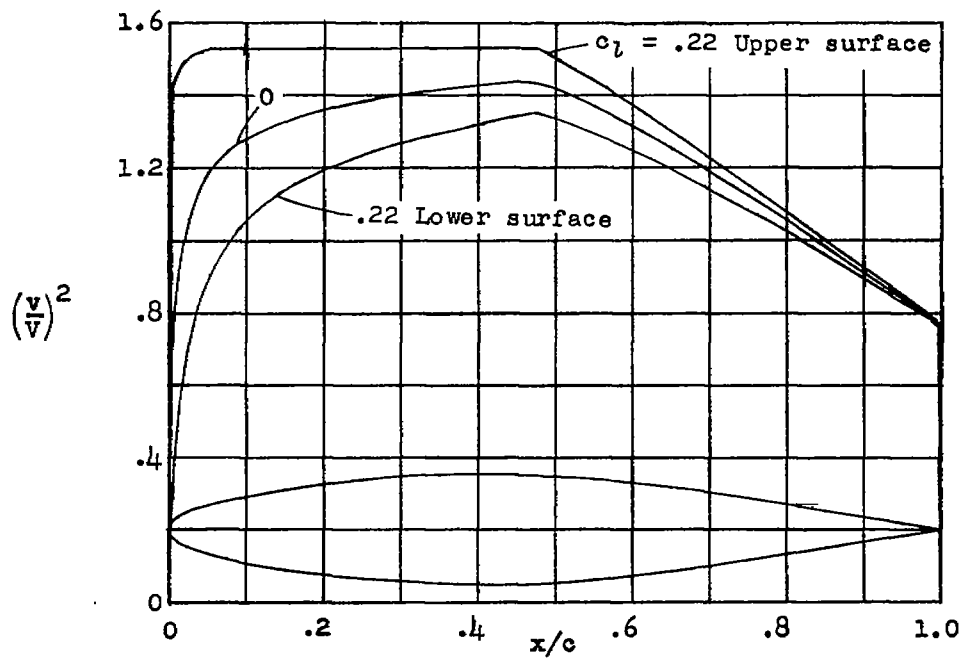
x (percent c)	y (percent c)	$(v/V)^2$	v/V	$\Delta v_a/V$
0	0	0	0	2.048
.5	1.131	.714	.845	1.586
.75	1.371	.781	.884	1.417
1.25	1.750	.891	.944	1.195
2.5	2.412	1.059	1.029	.880
5.0	3.255	1.187	1.089	.660
7.5	3.962	1.243	1.115	.553
10	4.553	1.280	1.131	.476
15	5.488	1.328	1.152	.382
20	6.198	1.359	1.166	.326
25	6.734	1.383	1.176	.282
30	7.122	1.401	1.184	.252
35	7.376	1.416	1.190	.227
40	7.496	1.427	1.195	.204
45	7.467	1.437	1.199	.181
50	7.269	1.419	1.191	.161
55	6.903	1.368	1.170	.142
60	6.393	1.311	1.145	.124
65	5.772	1.249	1.118	.109
70	5.063	1.186	1.089	.094
75	4.282	1.123	1.060	.080
80	3.451	1.056	1.028	.067
85	2.598	.986	.993	.055
90	1.743	.913	.956	.041
95	.887	.841	.917	.026
100	.032	0	0	0

L.E. radius: 1.446 percent c
T.E. radius: 0.038 percent c

Figure 16.-   NACA 65_2A015 basic thickness form.

NATIONAL ADVISORY
COMMITTEE FOR AERONAUTICS
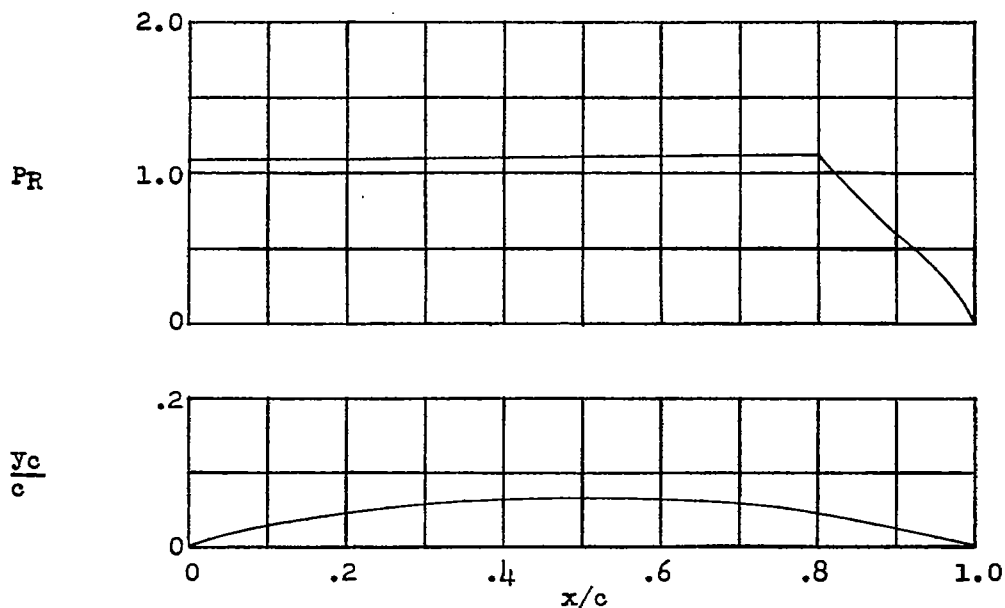
$c_{l_i} = 1.0$	$a_i = 1.40°$	$c_{m_{c/4}} = 0.219$		
x (percent c)	y_c (percent c)	dy_c/dx	P_R	$\Delta v/V = P_R/4$
0	0	-------	-----	-----
.5	.281	0.47539		
.75	.396	.44004		
1.25	.603	.39531		
2.5	1.055	.33404	1.092	0.273
5.0	1.803	.27149		
7.5	2.432	.23378		
10	2.981	.20618		
15	3.903	.16546		
20	4.651	.13452		
25	5.257	.10873	1.096	.274
30	5.742	.08595		
35	6.120	.06498		
40	6.394	.04507	1.100	.275
45	6.571	.02559		
50	6.651	.00607		
55	6.631	-.01404	1.104	.276
60	6.508	-.03537		
65	6.274	-.05887	1.108	.277
70	5.913	-.08610	1.108	.277
75	5.401	-.12058	1.112	.278
80	4.673	-.18034	1.112	.278
85	3.607	-.23430	.840	.210
90	2.452	-.24521	.588	.147
95	1.226	-.24521	.368	.092
100	0	-.24521	0	0

Figure 17.- Data for NACA mean line a = 0.8 (modified).

Fig. 18

0.20c simulated split
flap deflected 60°
R
▽ 6 × 10⁶
▽ Standard roughness
6 × 10⁶

R
◇ 9.0 × 10⁶
▢ 6.0
⊙ 3.0
△ Standard roughness
6.0 × 10⁶

R
◇ 9.0 × 10⁶
▢ 6.0
⊙ 3.0
△ Standard
roughness
6.0 × 10⁶

	R	a.c. position	
		x/c	y/c
◇	9.0 × 10⁶	.254	-.003
▢	6.0	.253	.014
⊙	3.0	.250	0

0.20c simulated split
flap deflected 60°
R
▽ 6 × 10⁶
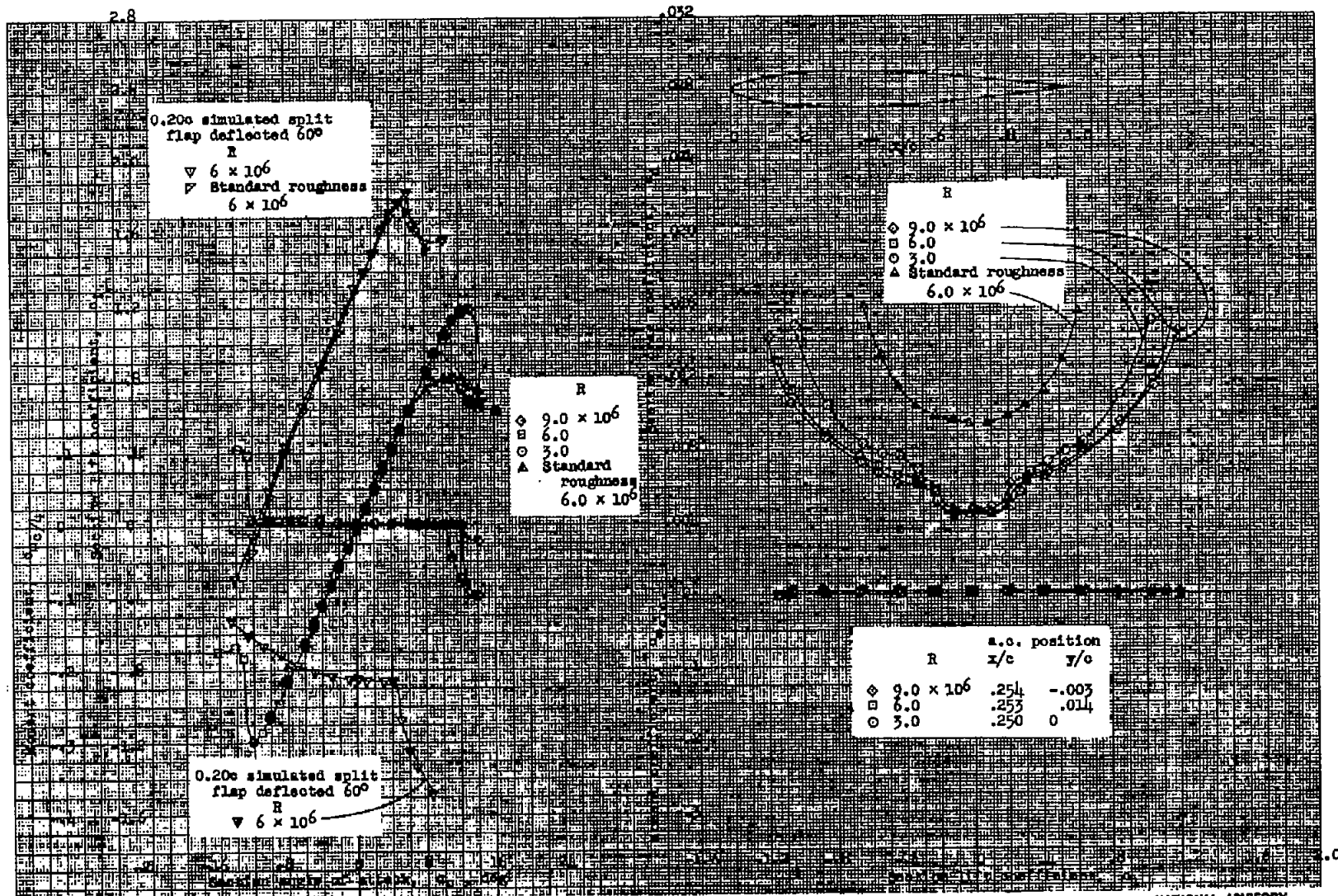
Figure 18.- Aerodynamic characteristics of the NACA 63A010 airfoil section, 24-inch chord.

NATIONAL ADVISORY
COMMITTEE FOR AERONAUTICS
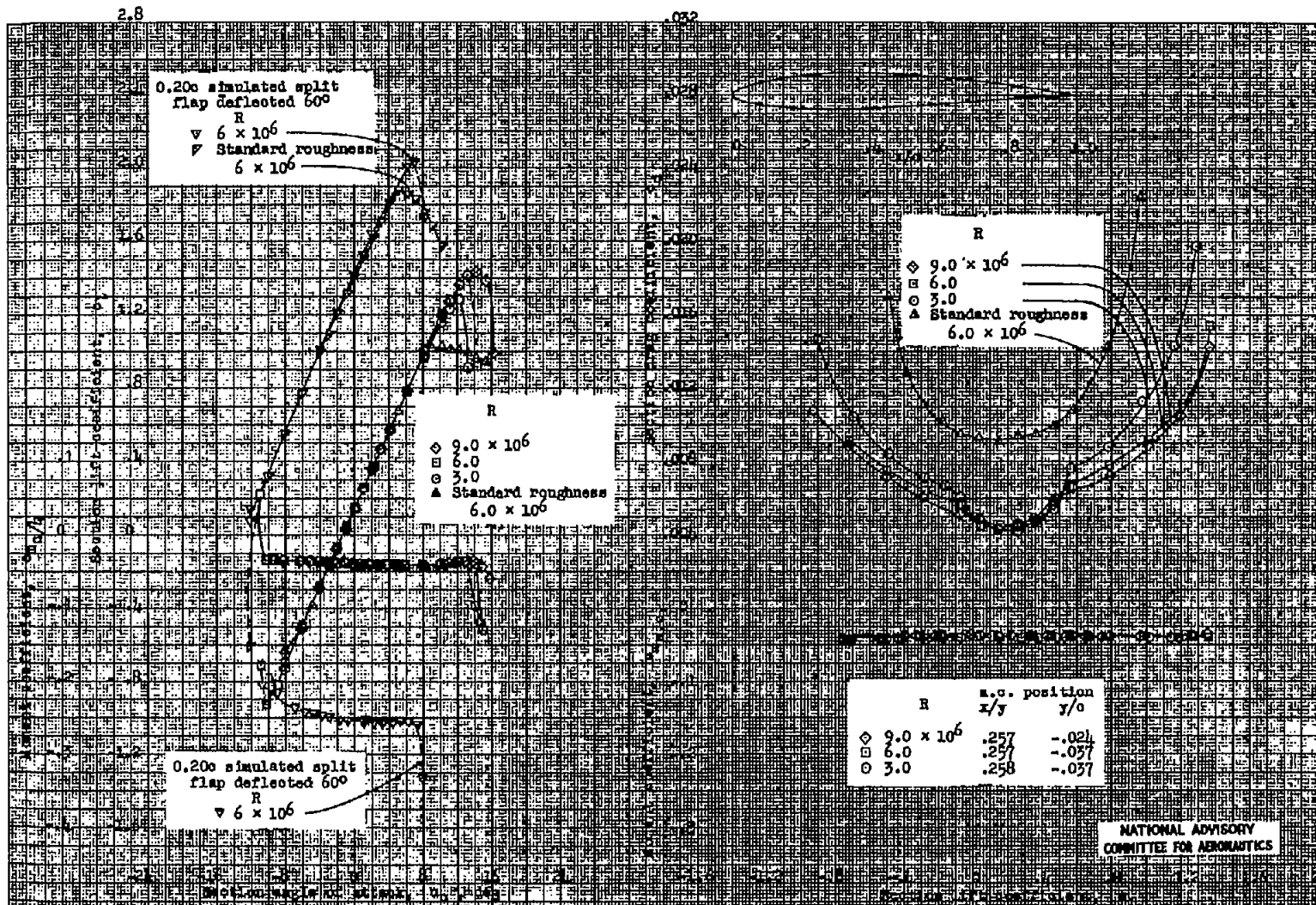
Figure 19.- Aerodynamic characteristics of the NACA 63A210 airfoil section, 24-inch chord.

Fig. 19

Fig. 20
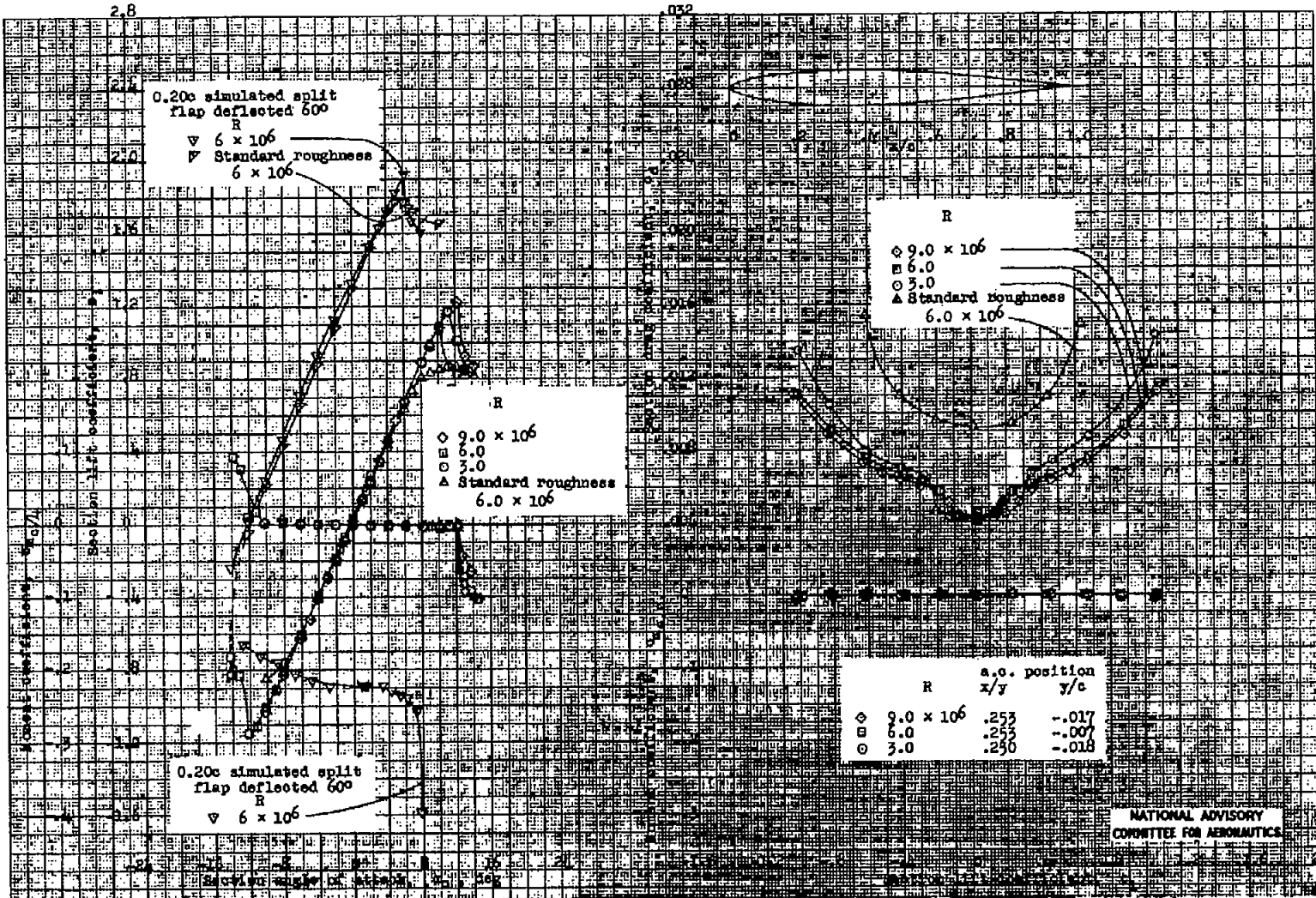
Figure 20.- Aerodynamic characteristics of the NACA 64A010 airfoil section, 24-inch chord.
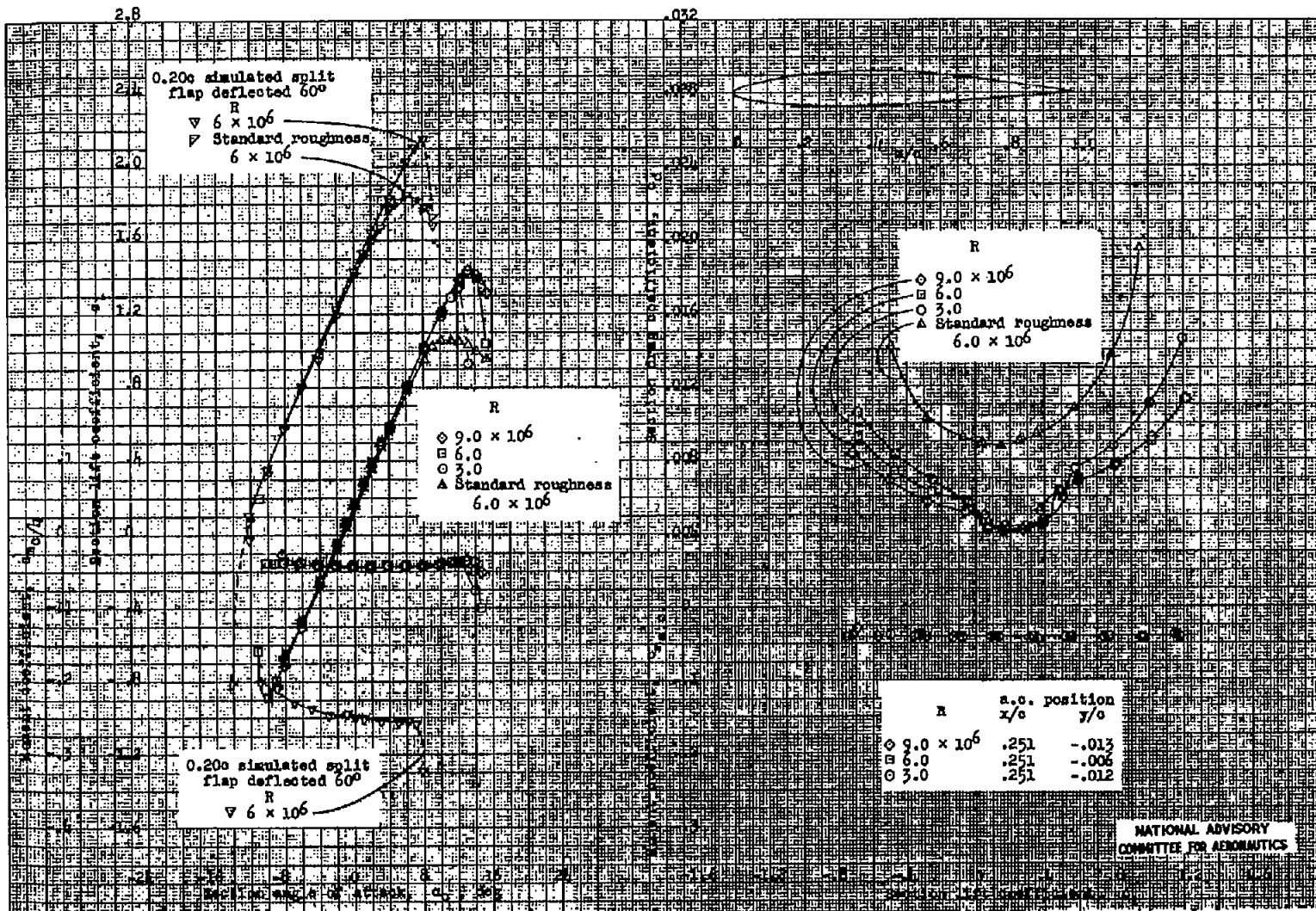
Figure 21.- Aerodynamic characteristics of the NACA 64A210 airfoil section, 24-inch chord.

Fig. 21
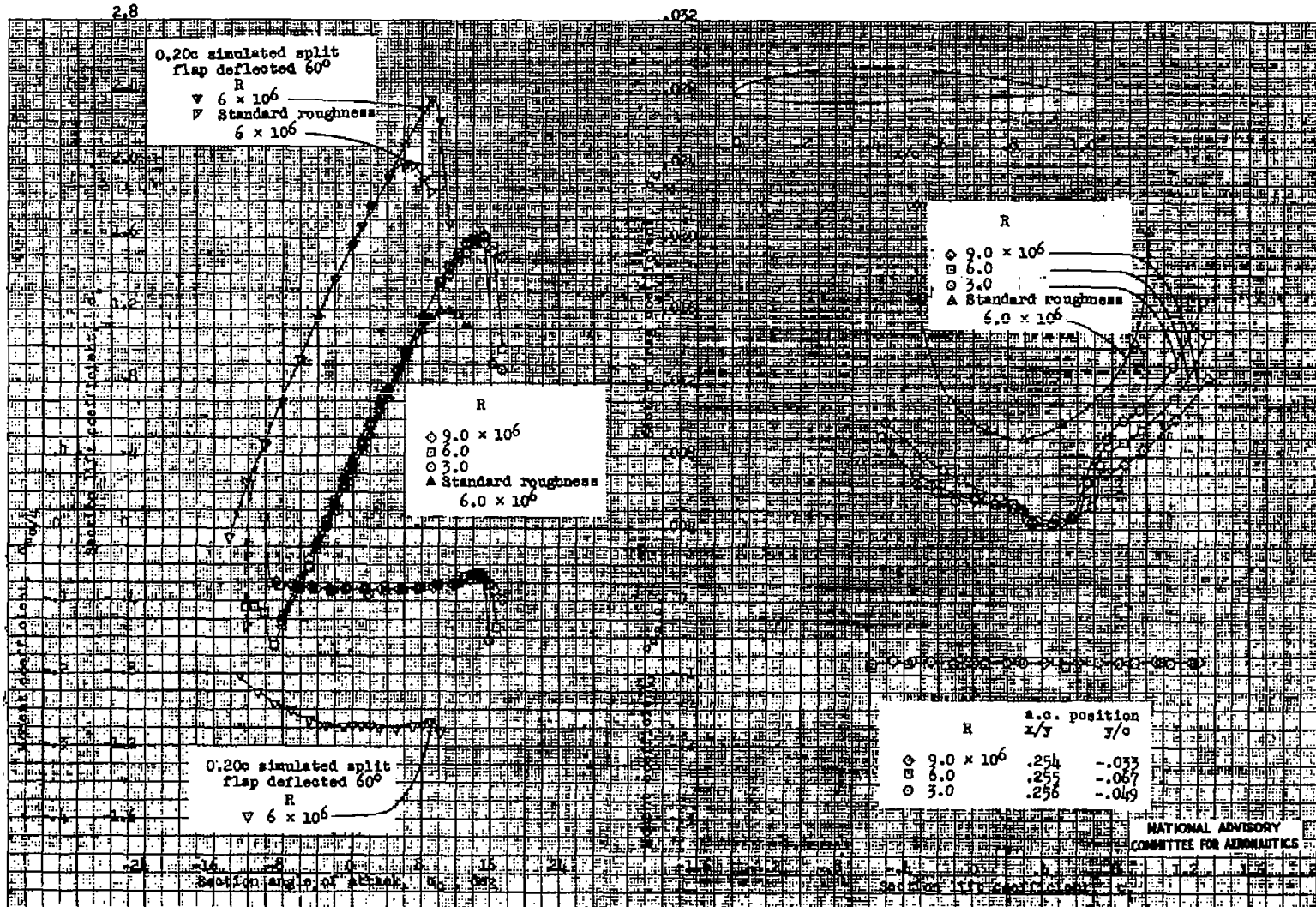
Figure 22.- Aerodynamic characteristics of the NACA 64A410 airfoil section, 24-inch chord.

Fig. 22

0.20c simulated split
flap deflected 60°
R
▽ 6 × 10⁶
▼ Standard roughness
6 × 10⁶

R
◇ 9.0 × 10⁶
□ 6.0
○ 3.0
△ Standard roughness
6.0 × 10⁶

R
◇ 9.0 × 10⁶
□ 6.0
○ 3.0
△ Standard roughness
6.0 × 10⁶

| | | a.c. position | |
R	x/y	y/c
◇ 9.0 × 10⁶	.252	-.021
□ 6.0	.253	-.030
○ 3.0	.254	-.048

0.20c simulated split
flap deflected 60°
R
▽ 6 × 10⁶

NATIONAL ADVISORY
COMMITTEE FOR AERONAUTICS
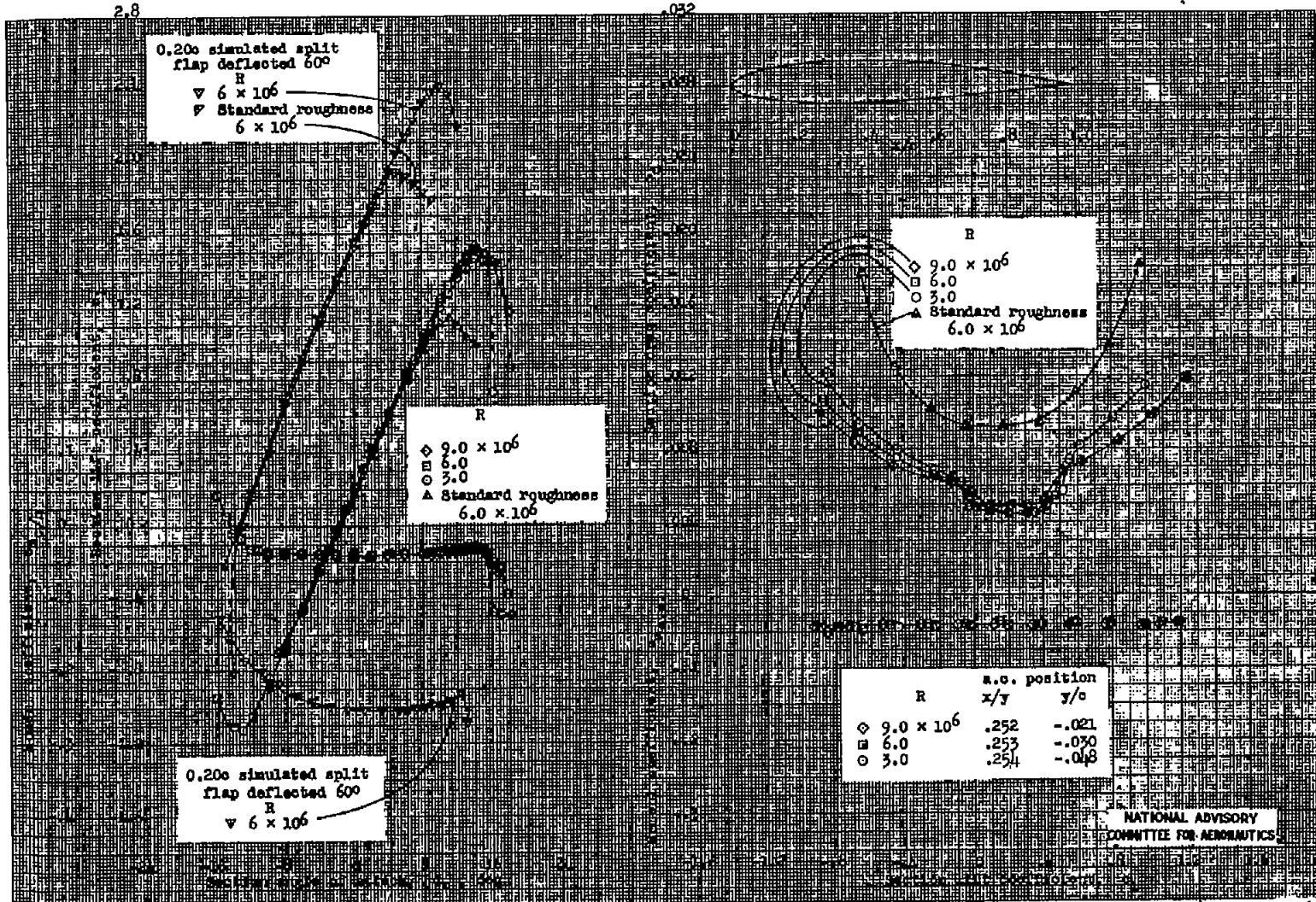
Figure 23.— Aerodynamic characteristics of the NACA 64₁A212 airfoil section, 24-inch chord.

Fig. 23

Fig. 24
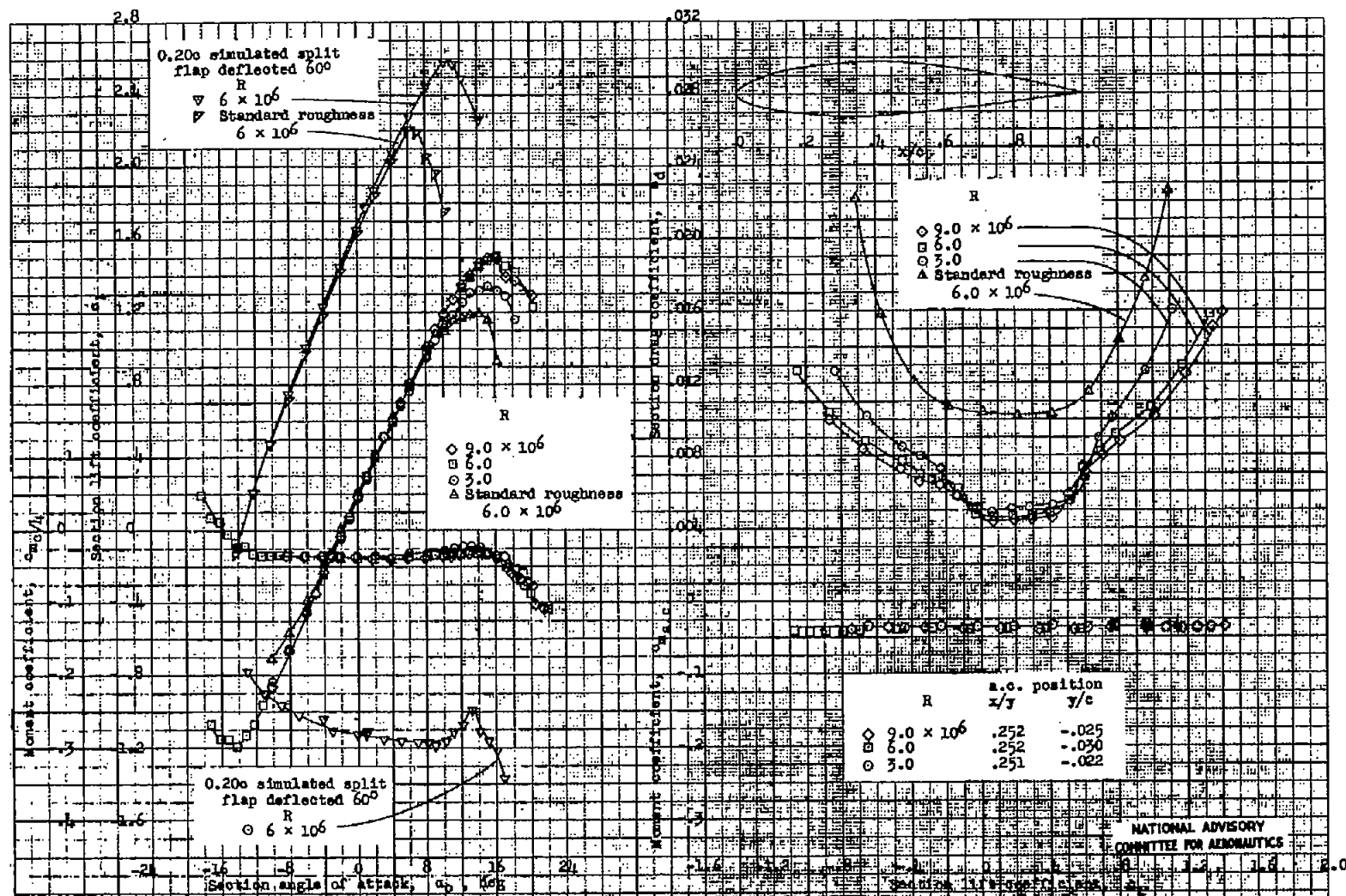
Figure 24.- Aerodynamic characteristics of the NACA 64₂A215 airfoil section, 24-inch chord.
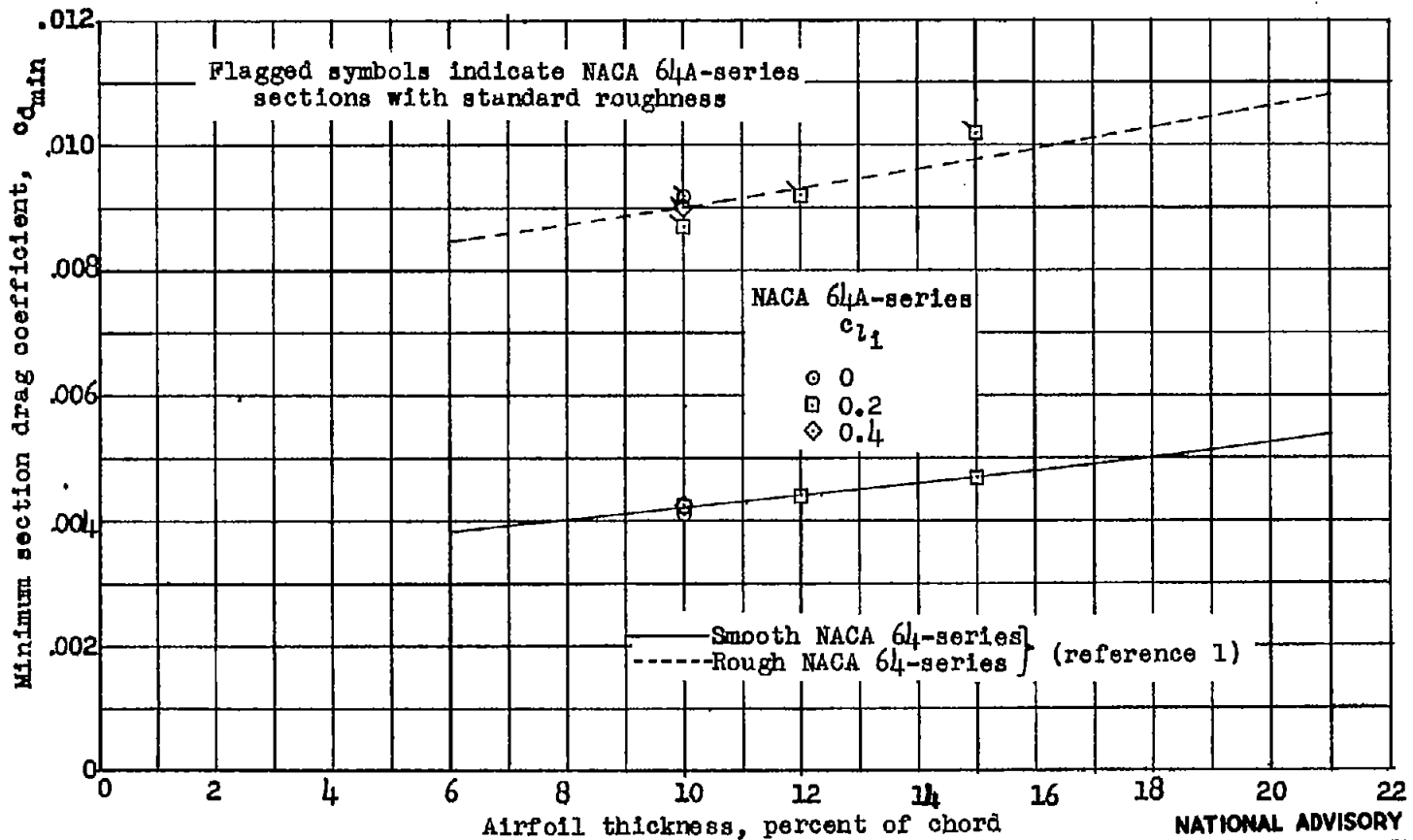
Figure 25.- Variation of minimum section drag coefficient with airfoil thickness for some NACA 64-series and NACA 64A-series airfoil sections of various cambers in the smooth condition and with standard leading-edge roughness. R, 6×10^6.

Fig. 25
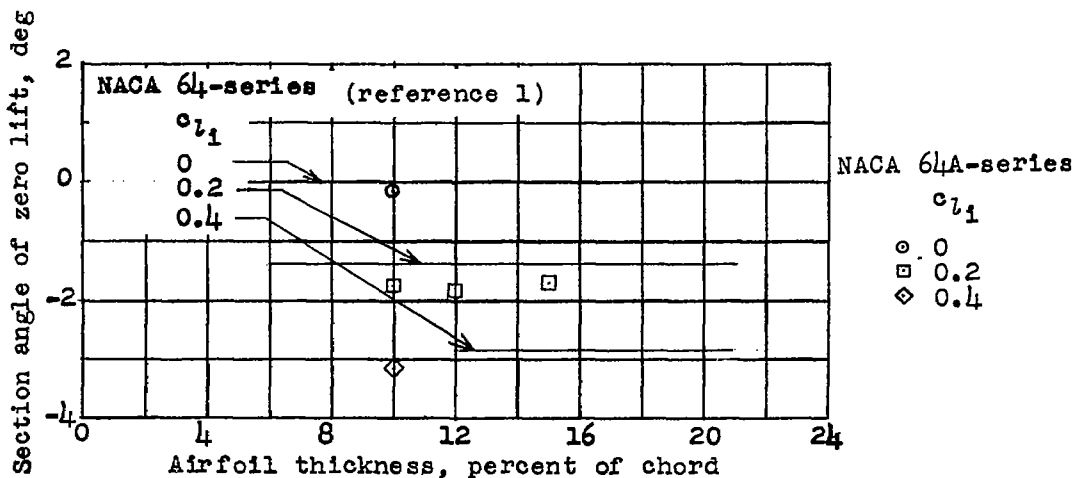
Figure 26.— Variation of section angle of zero lift with airfoil
thickness ratio and camber for some NACA 64-series and
NACA 64A-series airfoil sections. R, 6 × 10⁶.
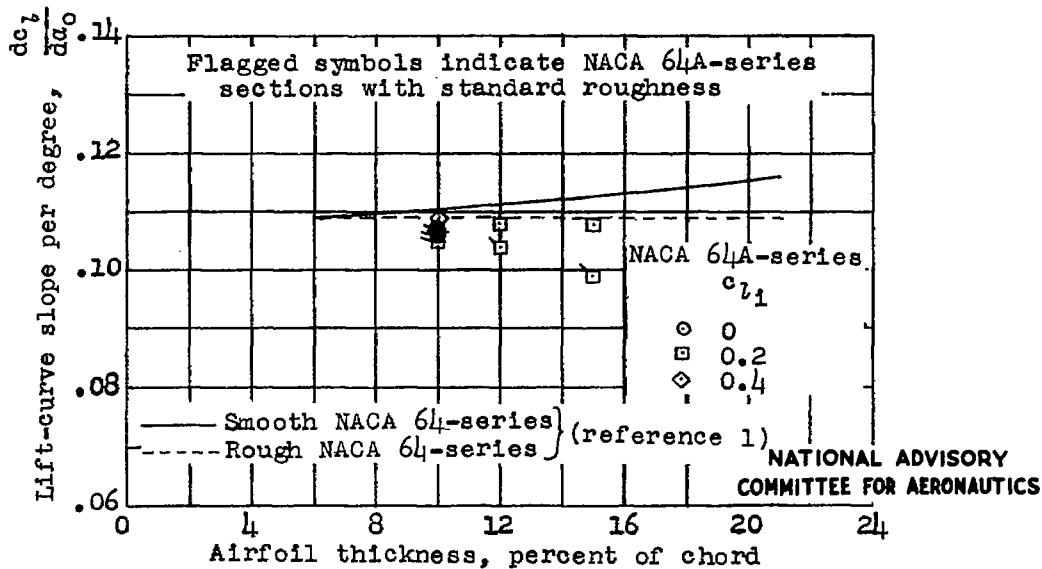
Figure 27.— Variation of lift-curve slope with airfoil
thickness ratio for some NACA 64-series and
NACA 64A-series airfoil sections of various cambers
both in the smooth condition and with standard
leading-edge roughness. R, 6 × 10⁶.
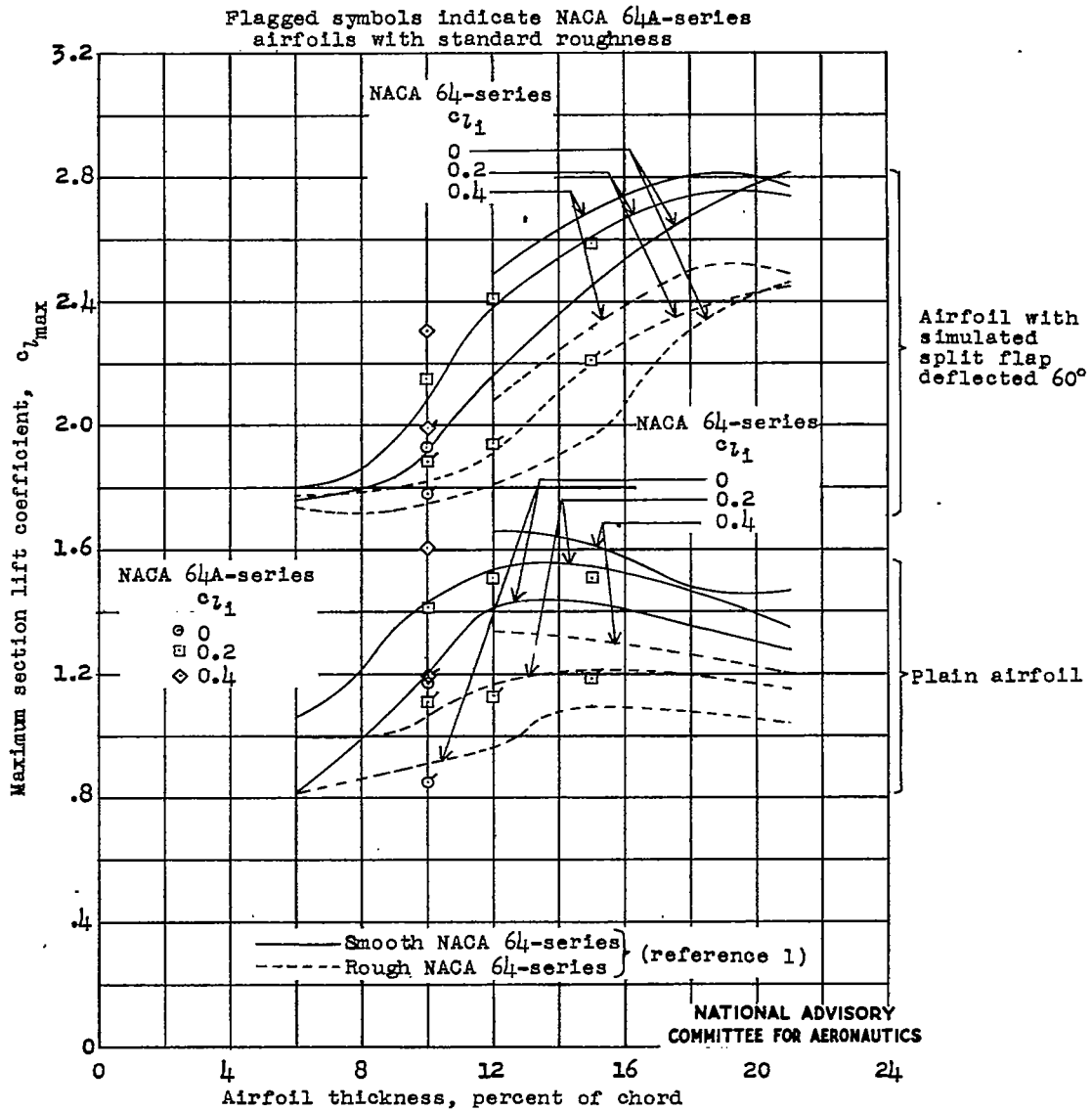
Figure 28.- Variation of maximum section lift coefficient with airfoil thickness ratio and camber for some NACA 64-series and NACA 64A-series airfoil sections with and without simulated split flaps and standard roughness. R, 6×10^6.
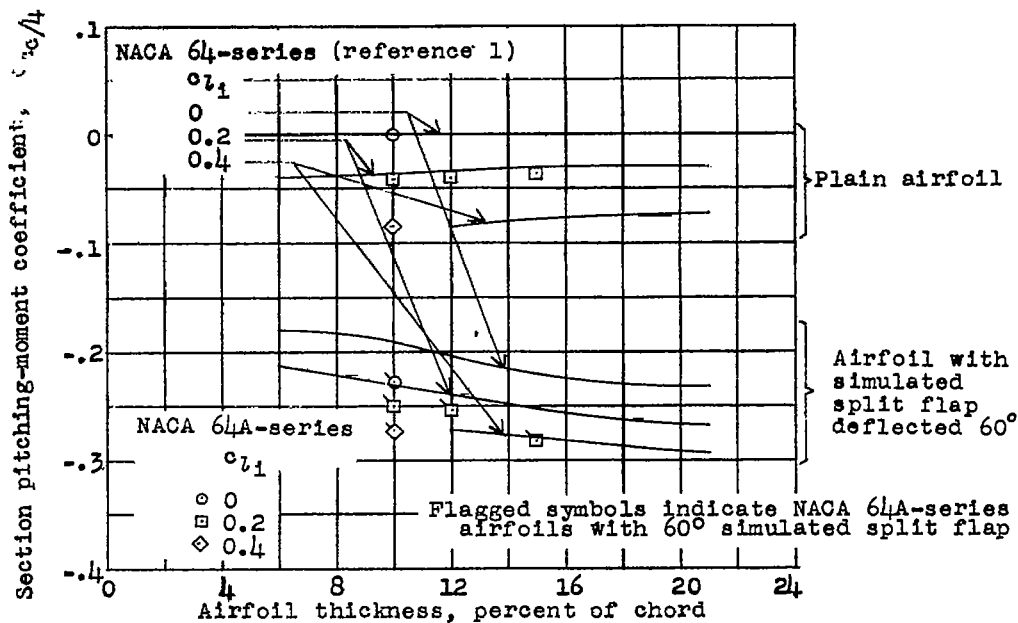
Figure 29.- Variation of section quarter-chord pitching-moment coeff-
icient at zero angle of attack with airfoil thickness ratio and
camber for some NACA 64-series and NACA 64A-series airfoil sections
with and without split flaps. R, 6 × 10^6.
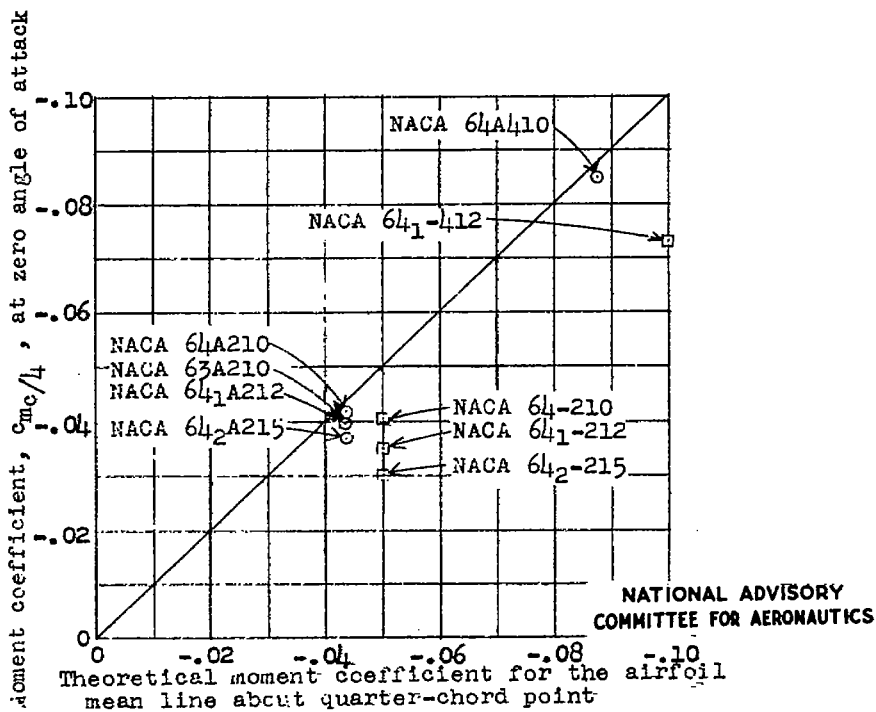
Figure 30.- Comparison of theoretical and measured pitching-moment
coefficients for some NACA 64-series and 64A-series airfoil
sections. R, 6 × 10^6.
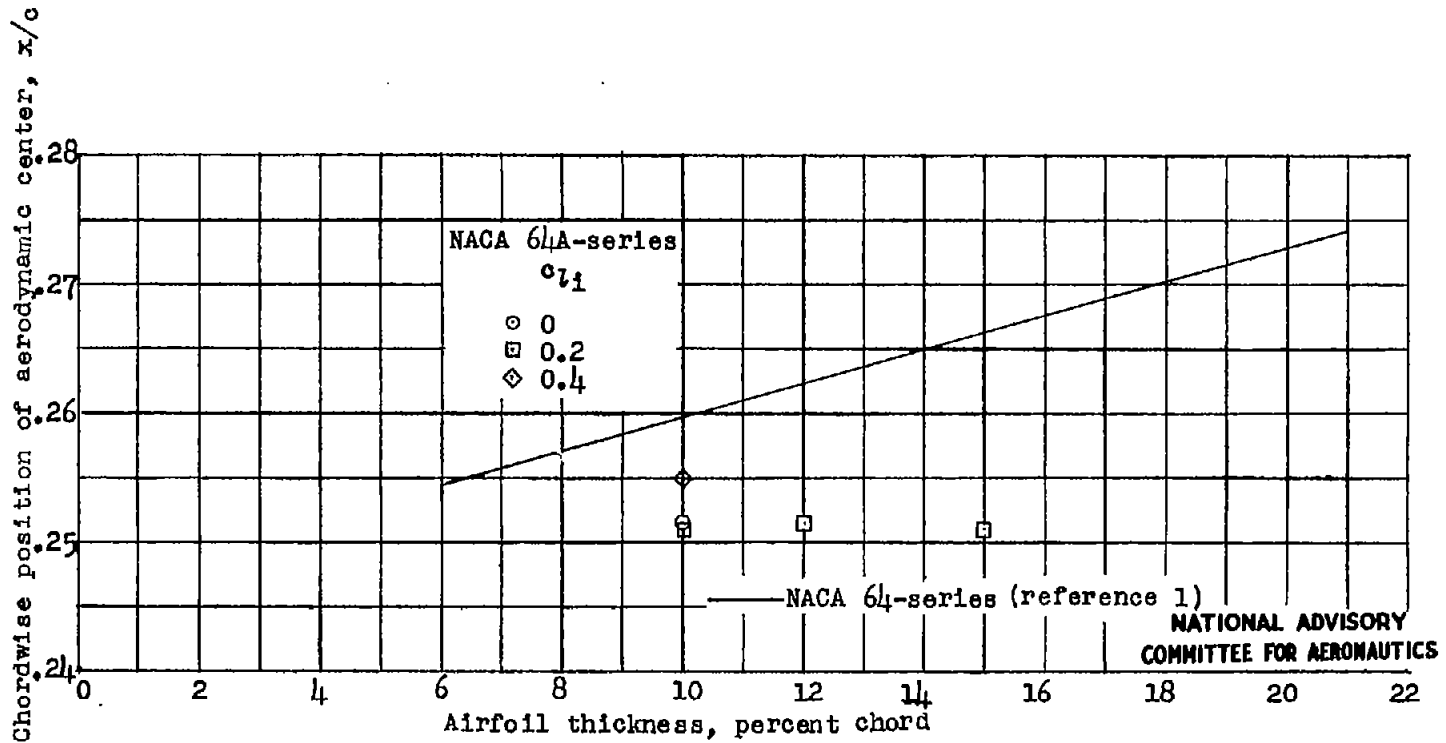
Figure 31.— Variation of chordwise position of aerodynamic center with airfoil thickness ratio for some NACA 64-series and 64A-series airfoil sections of different cambers. R, 6×10^6.

Fig. 31